2025-12-18

The Role of Dust Inputs and Sediment Phosphorus Diffusion Into Utah Lake, Utah, United States of America

Kristen E. Smith
Brigham Young University

The Role of Dust Inputs and Sediment Phosphorus Diffusion Into Utah Lake, Utah, United States of America

Kristen E. Smith

A thesis submitted to the faculty of
Brigham Young University
in partial fulfillment of the requirements for the degree of

Master of Science

Stephen T. Nelson, Chair
Joshua J. LeMonte
Barry R. Bickmore

Department of Geological Sciences

Brigham Young University

ABSTRACT

The Role of Dust Inputs and Sediment Phosphorus Diffusion Into Utah Lake, Utah, United States of America

Kristen E. Smith
Department of Geological Sciences, BYU
Master of Science

Human activities have led to excessive nutrient enrichment which is greater than lake systems can naturally assimilate. This process is known as eutrophication and it is driving significant algae growth resulting in the more common release of harmful toxins. Utah Lake, located in Utah County, UT is one such water body that even after major reductions in anthropogenic phosphorus influent, continues to experience frequent, harmful algal blooms. The extent to which natural processes, like atmospheric dust deposition and sediment recycling, contribute to the lake's phosphorus budget is still poorly understood.

To address this gap of knowledge, this study quantified phosphorus inputs from dust and analyzed porewater geochemistry from three lake sediment freeze cores. Dust collected with active air samplers showed no significant attenuation along the southwest–northeast transect as previously hypothesized, although phosphorus solubility declined in the same direction possibly indicating the significance of anthropogenic dust contribution. Porewater geochemistry revealed evidence of diverse porewater movement, exhibiting both groundwater-driven advection and diffusive release of phosphorus from the lake sediments. Using Fick's law, the estimated lake sediment diffusion contributes an average of 790 mT yr^{-1} (5.7 mg P m^{-2} d^{-1}), representing approximately 68% of total phosphorus loading to the lake.

These results highlight dust and lake sediment recycling as complex, understudied nonpoint sources of phosphorus. By clarifying their magnitude and mechanisms, this study advances understanding of nutrient dynamics in Utah Lake and informs for more effective strategies in eutrophication management.

Keywords: eutrophication, algal, water quality, atmospheric deposition, sediment flux

ACKNOWLEDGEMENTS

First and foremost, I would like to express my gratitude to my Heavenly Father for the opportunity to pursue and complete this Masters program. I would like to thank my committee chair, Dr. Steve Nelson, for accepting me into the program as well as mentoring me through this project. Your patience and experience have helped me immensely.

I'm grateful for the encouragement, feedback, and expertise of Dr. Barry Bickmore and Dr. Josh LeMonte. A special thank you to Kevin Rey for his skills and time driving the boat and helping with the equipment. I appreciate the support of the Wasatch Front Water Quality Council who funded this project and gave me firsthand learning experiences. Lastly, without my supportive husband (and kids), none of this would have been possible. Thank you for helping my dreams come true.

TABLE OF CONTENTS

LIST OF FIGURES

INTRODUCTION

Lakes naturally undergo a gradual evolution marked by sediment accumulation, decreasing water depth, and increasing biological productivity. Under natural conditions, this process, known as eutrophication, typically occurs over geological timescales (Schindler et al., 2016). Unfortunately, anthropogenic activities have accelerated lake eutrophication, leading to widespread health and environmental concerns (Ho et al., 2019). The excess nutrients trigger the rapid growth of algae, typically including cyanobacteria (blue-green algae), that decrease water clarity and frequently produce toxins (Paerl and Otten, 2013). These blooms cause ecological damage and pose health risks which is why they are called harmful algal blooms (HABs). Schindler (1974) found that phosphorus was the most important limiting nutrient (over nitrogen) in many freshwater lakes and that the management of this nutrient has successfully controlled HABs (Schindler et al., 2016).

Unlike other biogeochemical cycles, phosphorus relies primarily on the lithosphere as its source, meaning its initial release depends on the weathering of phosphorus-bearing rocks. The inherently slow pace of weathering allows the environment to maintain equilibrium between phosphorus release and deposition (Yuan et al., 2018). Once humans discovered the benefits of phosphorus as fertilizer, higher levels of phosphorus were released and have continued to overwhelm waterbodies worldwide (Bennett et al., 2001).

Point sources of phosphorus are relatively easy to track and regulate. These include municipal wastewater treatment plants (WWTPs), large livestock operations, urban stormwater, and streams. Nonpoint sources, which are often harder to quantify due to natural cycling and reuse of phosphorus, include upper watershed erosion, forests, groundwater, atmospheric deposition, stormwater runoff, and inputs from pastures. While management control of

phosphorus in WWTP discharge would seem the simplest to manage, these can be costly due to required major infrastructure improvements and may only address a small part of phosphorus loading to a given lake. Exploring natural inputs of phosphorus can provide insight into the probable effectiveness of regulatory decisions and what factors contribute the most to phosphorus addition. In other words, such studies provide information for making cost-benefit judgements for environmental management. In this thesis, the primary focus is on how the phosphorus in dust changes across the lake, as well as the mechanisms and release of phosphorus from lake sediment back into the lake.

STUDY AREA

This thesis used Utah Lake (UTL), Utah as a case study (Figure 1). UTL is an important economic and ecological entity in the region and has been an epicenter of metropolitan growth in recent years (Harris, 2023). Concerns about the health of the lake became acute in October 2014, when a pet death occurred after an outing to the lake. News outlets assumed neurotoxins from a HAB as the cause death, but given the quick breakdown of neurotoxin molecules, it could not be confirmed ("FOX 13 News Utah (KSTU)," 2016). The Utah Division of Water Quality used this story as evidence to support new statewide phosphorus regulations that included the seven WWTPs that discharge to UTL in hopes of lessening HABs (Utah Division of Water Quality, 2014). By 2019, upgrades had cost adjacent cities in Utah County at least $300 million (Hoffman, 2019), and effluent-phosphorus concentrations had been reduced by nearly half and continue to decline as additional upgrades are completed. Yet HAB hotspots still exist due to persistent elevated lake phosphorus concentrations, reduction of lake surface area and increase in water temperatures (Tate, 2019). Numerous studies have been done to quantify natural

phosphorus additions (see section 1.2), but further studies are needed to limit the uncertainty and verify contribution estimates.

UTL occupies more than a quarter of Utah Valley acreage, with an approximate surface area of ~380 km^2 (Jackson & Stevens, 1981). This basin lake lies between the Wasatch Mountains, which comprise the eastern edge of the Basin and Range province, and the Lake Mountains to the west (Figure 1A). While the shallow average depth of 2.8 meters (Fuhriman et al., 1981) makes this freshwater system naturally eutrophic, human influence in conjunction with climate change has gradually led to water quality concerns. Land use surrounding UTL is primarily irrigated agricultural or urban areas leading to a significant anthropogenic contribution of nutrients (Figure 2) (Utah Division of Water Resources, 2014).

UTL water has notably less clarity than other lakes in the state. This is primarily due to the precipitation of calcium carbonate particles, algae growth, and sediment resuspension common in shallow lakes (Fuhriman et al., 1981). Wind, waves, and changes to the lake surface area have notable impact on the amount of suspended sediment in the lake. Due to the invasive common carps' bottom feeding habits, the bottom living layer of the lake (periphyton) has been decimated allowing sediment and nutrient resuspension (Matsuzaki et al, 2007).

With the semiarid climate of northern Utah, direct precipitation only contributes a small amount of inflow to UTL (15%). Snowpack runoff from the surrounding mountains is the main source of water to UTL, by means of streams and groundwater (PSOMAS & SWCA, 2007). Streams contribute about 51% of the inflow with the largest contributions being from the Provo River (from the east) and Spanish Fork River (from the southeast) (PSOMAS & SWCA, 2007) (Figure 1A). Other surface inflow accounts for 10% and groundwater/ springs contribute the remaining 24%. Evidence of this groundwater influence is widespread throughout the lake,

where warm, saline springs have produced tufa and travertine structures and deposits (Baskin et al., 1994). The most prominent of these deposits form Bird Island (BI), the only island in Utah Lake, which is sufficiently large to emerge above the lake surface and whose exposed area varies greatly with lake level (Figure 1B).

Like Great Salt Lake (GSL), UTL is a remnant of Lake Bonneville, which filled large areas of the eastern Basin and Range province between 30 ka and 12 ka (e.g., Oviatt 2015). UTL still connects to GSL today through its only stream outlet, the Jordan River (Figure 1A). The Jordan River flows from the northwest corner of UTL to GSL and contributes to 51% of UTL outflow. Remaining water leaves the lake through evaporation (42%) or seeps from the lake into the underlying groundwater system (7%) (PSOMAS & SWCA, 2007).

Southwest of UTL is another remnant of Lake Bonneville, Sevier Lake. Unlike the GSL, Sevier Lake no longer has a hydrologic link to UTL, but it is a significant source of dust to the Utah and Salt Lake Valley areas (Figure 1C) (Goodman et al., 2019). Sevier Lake has mostly been noted as a dried lakebed, or playa, since the mid to late 1980's, due to irrigation diversions along the Sevier River. Strong seasonal, southwesterly winds entrain playa particles, producing considerable dust deposition events (DDEs) about 4-5 times a year (Hahnenberger & Nicoll, 2012). On a more local scale, recent research concluded dust from agricultural activities on the fields south and west of UTL to be more of a dust source (Telfer et al., 2023).

SUMMARY

This thesis is organized into two chapters. Chapter 1 will address knowledge gaps regarding atmospheric deposition of dust such as attenuation results across the lake and extending previous research conducted regarding lake water dust reactions (Hu 2025). Chapter 2 focuses on the internal sediment recycling of phosphorus, specifically examining phosphorus

mobilization from porewater and its implications for sustaining elevated water column concentrations.

CHAPTER 1: Dust Collection Study

Atmospheric deposition (AD) has been a focus in recent research to better quantify natural inputs of phosphorus into UTL. This chapter will fill in knowledge gaps on dry AD of dust.

1.1 PREVIOUS WORK

Researchers have tried to understand where dry AD, or dust, originated and if it had a noteworthy influence on the phosphorus addition. Goodman et al. (2019) first concluded 90% of the dust in the north Utah region is sourced from modern playas or exposed lake beds (e.g., Great Salt Lake desert, Sevier Lake playa and other valley bottoms that may host ephemeral lakes). Dust storms in early spring were found to bring in a significant amount of dust. Unfortunately, phosphorus content was not explicitly examined in this study.

Brahney (2019) prepared a report for the Utah Lake Science Panel and the Utah Division of Water Quality to go more in-depth on the potential contribution of dust to UTL. Data used was from regional AD samplers located at high elevation sites in Colorado, Wyoming and the Eastern Uinta Mountains. Moreover, the calculations of AD were based on the attenuation of road dust mobilized by highway traffic adjacent to the southern shoreline of Lake Tahoe (VanCuren et al., 2012). Cole et al. (1990) measured insect and plant parts sourced from the forest surrounding a lake as part of an estimation of total AD to a small lake in New Hampshire. Plant and animal parts dominated the deposited phosphorus, although attenuation included an approximate 80% decline within about 25 m from shore. Notably, a comparison of "wet" vs "dry samplers indicted that wet samples collected about 15 times more phosphorus than dry samplers. With these studies in mind, Brahney (2019) calculated based on average grain size distributions for local and urban dusts indicate a deposition rate of 93.6 mg TP m^{-2} yr^{-1} across the UTL area. Distributing this

across the surface area of the lake means about 35.6 mT-P/yr. Fieldwork was then needed to confirm the calculations.

Olsen et al. (2018) used a traditional collection method, like that instituted by the National Atmospheric Deposition Program, to collect wet/ dry AD around UTL. The data collected were then used to create interpolated deposition of phosphorus addition across the lake. This study concluded that AD is a significant contributor of total phosphorus, with an upper and lower bound of 8 to 350 t yr^{-1}. The high value was a true estimation of total AD with outliers not removed while the low value was estimated by not only removing samples that contained plant or insect parts but also removed samples that containing even the smallest visible particle of dust from the dataset.

Barrus et al. (2021) modified the methods of the previous study, noting that the assumption of Olsen et al. (2018) for attenuation of dust across the lake may be skewed due to potential anthropogenic inputs such as unpaved roads or agricultural fields and that more than 43% of collected samples in the study were labeled as contaminated with insects, etc. Barrus et al. (2021) added AD data from Bird Island (BI) as a mid-lake location, where their findings suggested that AD rates were not statistically higher than those from shoreline samplers during the sampling period. This study measured AD over a two-year period (2019 and 2020) with the July to November 2020 samplers fitted with a 500 μ mesh screen. Using updated Kriging methods, they concluded that total phosphorus estimates were a bit lower than Olsen et al's (2018), with estimates for non-screened samplers being 262 (2019) and 133 t yr^{-1} for 2020.

Tefler et al. (2023) built on the work of both Goodman et al. (2019) and Barrus et al. (2021) to examine the amount of local dust contribution and concluded empty fields south and west of the lake were a major source of the dust portion of AD onto UTL.

Based on previous studies, this thesis fills important gaps in the natural input of phosphorus by examining both dust weights and phosphorus solubility on and around UTL. It extends the work of Hu (2025) by including active dust sampling on BI, which is about 3 km from the nearest shoreline. Thus, it gives a sense of the magnitude of attenuation around UTL.

1.2 METHODS

1.2.1 Filter Collection

Following the methods utilized by Hu (2025), three MiniVol TAS Portable Air Samplers were installed to capture dust depositing on or near UTL (Figure 3). The MiniVol samplers proved ideal to reduce or even eliminate contamination from insects and birds hypothesized by others (Utah Department of Environmental Quality, 2025). The same Provo High School (PH) location as Hu (2025) was monitored and this study added a mid-lake location at Bird Island (BI) and a southwestern shore location at Mosida Handcart Trek Camp (M). The alignment of the air samplers was based on the substantial amount of dust added from that direction during DDE (Steenburgh et al., 2012). Due to the higher lake level of the 2024 water year, sampling began in July and ended in October 2024, where weather conditions prevented further sampling.

Using a pre-weighed, EPA-compliant, 2µm PTFE 46.2 mm filter (40 CFR Appendix L to Part 50 - Appendix L to Part 50, n.d.), the MiniVol Air Samplers ran with a continuous flow rate of 5 liters per minute. This method, used by Marcey et al. (2024), allowed the air samplers to give an idea of the nature of dust deposited minus the impacts of birds and insects. However, it is difficult to represent dry AD available from passive samplers. Filters were changed bi-weekly (weather permitting) to allow for sufficient dust accumulation for analysis (Hu, 2025). A total of 18 filters were collected representing 6 data periods from 7/10/24 to 10/15/24.

1.2.2 Filter Analysis

Prior to initial weighing and following sample collection, filters were placed in a desiccant jar for 24 hours to eliminate adsorbed moisture. Filter weights were compared to study the quantity of dust that was making it across the transect of the lake defined by these three air samplers.

To investigate the mineralogic associations of phosphorus within the dust, three filters were analyzed using an Apreo C Low-Vacuum Scanning Election Microscope (SEM) at BYU's Electron Microscopy Facility. Energy dispersive x-ray analysis (EDXA) was used to create elemental x-ray dot maps on the electron backscatter images. Two filters, an otherwise unanalyzed 2023 filter (Timpanogos Special Service District) collected by Hu (2025) and a 2024 Bird Island filter from this study, utilized low vacuum mode without a coating to help with controlling charging artifacts. These two filters helped set a qualitative baseline for phosphorus occurrences in dust, but the low resolution and elemental mapping time made it difficult to correlate the elemental data with specific particles. Thus, the third filter, a 2023 Provo High (PH) filter collected by Hu (2025), was coated with gold/palladium (80:20) to reduce charging artifacts while using high vacuum mode and provided better resolution for a more thorough qualitative analysis.

The 2023 PH filter was chosen specifically due to the out of norm PM10 levels during the two-week sample period. A monitoring station in Lindon, Utah was used as a proxy for Utah County air quality and data were obtained for November 2023 (Utah Department of Environmental Quality-Air Quality, 2023). Later investigation showed that while there were no strong southwest winds during that time, high pressures in the area were causing inversion

conditions, meaning that trapped pollution was likely influencing the particulates observed on the filters.

For geochemical measurements, the weights were recorded again after being in laboratory air for 48+ hours. Each filter and one blank (n=20) was placed into a Teflon beaker with 20 mL of synthetic lake water to determine the amount of lake soluble phosphorus. Samples were mechanically shaken for 24 hours and then placed on an inclined surface to allow particulate settling. The water was carefully decanted, filtered through a 0.45µm filter and acidified with 1 mL of trace metal grade nitric acid to keep ions in suspension. Major cations were measured using a ThermoFisher iCAP 7400 Duo inductively coupled plasma optical emission spectrometer (ICP-OES). Specifically, the increase in phosphorus levels compared to the blank synthetic lake water suggested by Hu (2025) was examined. A larger panel of trace metals was also determined.

The remaining water and dust in the Teflon beakers were allowed to dry and reweighed to determine the remaining dust weight, noting that the calculated masses included trace amounts remaining from the synthetic lake water solution. Then, 4.8 mL of a 3:1 HNO3/ HCl mixture was added to each sample to digest the remaining dust. These samples were placed on a hot plate at 100 °C for one hour and rinsed with 15.2 mL deionized water into another tube, to allow for centrifugation. After centrifuging, no other dilutions were made, and the samples were run on the ICP-OES for total cation analysis. After correcting for weight and solutions added, the blank was used to subtract and correct leftover solutes.

1.3 RESULTS AND DISCUSSION- Filter Analysis

In this section the data collected was used to assess the following:

- Wind direction at each air sampler was assessed to determine the likely daily source of dust for that sampler.
- Dust weight was compared across the air samplers to determine if it was attenuated between shore and mid lake locations.
- Based on attenuation results, total dust solubility across the sites was examined to increase insight into bioavailable phosphorus fractions.
- Phosphorus elemental relations in the dust were assessed using SEM elemental mapping as well as qualitative examination of the dust particles.

1.3.1 Wind Direction

Tefler et al. (2023) reported 5-year wind roses using data from the Utah Fruit Growers Association weather stations, but for the short scope of this project, those wind roses proved inconclusive due to the varying directions of the low wind speeds and proximity to topographic features that may have affected wind directions. Instead, two MESOWEST weather station locations, UTLAK and PVU, provided the data (Figure 3) and wind rose diagrams were made for each station for the sample period (Figure 4). The southwestern side of UTL primarily experiences a northeast wind direction, while the eastern side of the lake sees strong southeast winds. Typical Utah canyon winds can exist in the morning hours, but even with removing data collected between 3 am and 9 am, the prevailing wind directions remained the same for both locations. During data analysis, wind data also showed that these weather stations more often experienced opposite wind directions (again possibly due to topography) rather than the same wind direction. When the wind directions were the same, they were more likely to be from the southwest. When the winds were different, it was common to see west winds on the east side and east winds on the west side. This is most likely due to the topography of West Mountain

impeding slower winds, while higher wind speeds allowed alignment in the southwest direction. In conclusion, during this sampling period M is probably not a dust source in everyday dust deposition for BI and it would be better to assume that the Lincoln Beach (LB) area studied by Hu (2025) is a better dust source that moves toward BI and then PH.

1.3.2 Filter Weight

Local researchers have hypothesized that attenuation of dust, or the attachment of windblown particles to the lake surface, leads to a significant addition of dust to the margins but not the interior of the lake (Utah Department of Environmental Quality, 2025). To evaluate this, the filter weights over time were compared. Although LB may be a better source for BI dust, this sampler was not active. However, because the M air sampler was in an area with similar land use to that of LB (mostly agricultural or state lands) it was treated as the origin for dust approaching the lake, and a comparison of dust weight was taken moving northeast across the lake. BI represented a mid-lake point and PH represented the final northeast location.

Filters were compared using dust weight per running time to correct for collection time variances. Figure 5a shows dust weights per day at each site plotted against date collected. PH more often exhibited the highest weight overall while M and BI interchanged from mid to lowest weights. If attenuation were significant, the expected result would be PH having the lowest weight since it is at the end of the fetch across the lake. Comparing overall accumulation of dust with Hu's (2025) results from 2023, BI fell within the results of the other stations and again did not signify attenuation.

To check the statistical significance of the filter weights across the lake, data was normalized by dividing collection time for each dust collection date and plotted it against the distance

northeast from M (Figure 5b). The null hypothesis was that there is no change in time-normalized dust weight deposited with distance along this trajectory. That is, the slope of the normalized dust weight versus distance traveled in the NE direction is indistinguishable from zero. The slope was calculated to be 0.0073 ± 0.0081, which encompasses 0, indicating that the slope is statistically indistinguishable from 0 at the 95% confidence level. Ultimately, there was no significant evidence of dust attenuation along the NE trajectory from M to PH during this sampling period.

1.3.3 Filter Geochemistry

A synthetic lake water extraction was used to determine the amount of soluble phosphorus in the dust, while an aqua regia digestion determined the total remaining amount of phosphorus. After correcting the synthetic lake water and acid digestion for the dust weight in each sample, a percentage of soluble phosphorus was calculated for each sample (Figure 6a).

Members of the Utah Lake Science panel have questioned the validity of using BI as a mid-lake location for atmospheric deposition due to the number of birds that inhabit the island in warm months where bird dust/dander, feathers or droppings have been thought to disrupt the samplers (Utah Department of Environmental Quality, 2025). The active air samplers used in this project prevented the contaminations mentioned and due to the higher water year during the sample collection period, substantial amounts of birds previously seen were not present. A trail camera was deployed with the air samplers and determined birds were not landing on the air sampler tower. One filter from BI did have a notable microscopic feather, though this is thought to be insignificant due to the lack of significant phosphorus from such a source.

Two notable patterns were found in the data: first, the BI filter solubility gradually increased throughout the sample period and second, PH and M seemed to rise and fall in tandem. BI tended to have a mid to lower mass accumulation than PH and M but had a higher phosphorus solubility. One explanation could be that wind speeds were generally low enough that smaller particles, like clay fractions, were making it across the lake and tended to have a higher solubility of adsorbed phosphorus. Of important note is that the PH filter was placed higher than the other air samplers on top of the full-size stadium bleachers (about 14 m above the ground). A possibility could be by the time dust arrived at the PH site, other dust caused by anthropogenic activities (construction or street dust) could have been added to the filter, decreasing the solubility percentage. Alternatively, if attenuation is happening, the soluble phosphorus particles could have dropped out before arriving at PH.

The second notable pattern where M and PH have similar temporal solubility trends is interesting because of the above noted differences in everyday wind direction. M could be higher due to the amount of agriculture in the area and applied fertilizer, but overall, wind directions and sources are responsible for the phosphorus addition to the lake. In other words, the times with similar wind directions could be the larger source of phosphorus that affects areas all around the lake.

In following the same statistical method as present for time-normalized filter weight, a time-normalized solubility comparison was created across the lake (Figure 6b). This graph does show a significant statistical slope as it does not include the null hypothesis of a slope of zero. This means that from M to PH there is a statistically significant decrease in solubility from the SW to NE direction across the lake. This could be another indication of anthropogenic influence on the

amount of dust, while BI is only collecting total mid lake dust which is perhaps finer and more soluble.

1.3.4 Scanning Electron Microscopy

After analyzing two filters, T 2023 and BI 2024 under low vacuum conditions (Figure 7a and 7b), the third filter, PH2023 imaged at high vacuum provided clearer particle data for qualitative analysis (Figure 7c). For fluorescent X-rays, there are possible spectral interferences with the gold coating, but phosphorus hotspots were observed. The use of high vacuum also reduced previously experienced sample drift and increased image quality.

Site 2 on the PH2023 filter was noted as having a significant phosphorus hotspot (Figure 8a). Two or three small phosphorus hot spots were common on the other filter sites, but a particle of this size had not been seen previously. Weather analysis for the time this filter was deployed showed that it was a period of heavier inversion conditions. During inversions, emissions and airborne particulates are trapped close to the ground, most likely enhancing local dust with pollutants before deposition. Munroe et al. (2025) showed that phosphorus, although on the lower end, was among the enriched elements in urban dust, versus downwind dust.

Specific mineralogy was not conducted on this filter, but Hu (2025) noted that during the sampling period, PH exhibited overall higher clay percentages compared to the other sites. While the instrument phase identification software did not produce any conclusive results to identify individual phases, manual elemental overlay map tracing provided additional insight (Figure 8b). From the overlay mapping, one can see that the primary element correlating with the phosphorus hotspots is calcium. Because dust is a conglomeration of multiple particles, a possible correlation with magnesium and chloride was also observed on the primary phosphorus area. Knowing

exactly where the phosphorus exists is beyond the ability of this analysis due to excitement of fluorescent X-rays from nearby particles. This along with particle topography makes exact phase identification difficult.

In the future, SEM analysis of filters will be productive coupled with XRD and ICP analysis. This would mean two air samplers would need to run at the same site for the same period so one filter could be coated for high vacuum SEM analysis. The number of mapped sites would need to increase to obtain a better sampling of the filter and determine if the large particle found at site 2 of PH 2023 is important and how much of the phosphorus present on filters is represented by large versus small particles. Shorter filter collection time could possibly provide correlation of amount/ type of phosphorus based on weather conditions (fireworks vs. discrete dust event vs. inversion).

1.4 CONCLUSIONS

- Daily wind accounts for the main addition of dust seen on Bird Island. Agriculture in the south/ southeast would be the primary activity producing daily dust.
- No significant evidence of dust attenuation was seen along the northeast trajectory from M to PH during this sampling period.
- There is a statistically significant decrease in solubility from M to PH (southwest to northeast) potentially due to anthropogenic influence on the dust.
- SEM showed a strong calcium correlation with phosphorus in the dust, but more SEM study would help in correlating mineralogy, elemental mapping, and solubility.

CHAPTER 2: 2024-2025 Lake Sediment Freeze Core Study

2.1 PREVIOUS WORK

Abu-Hmeidan et al. (2018) characterized the total phosphorus (TP) in present lake sediment (top 4 inches) to sediment samples outside the lake. They concluded that anthropogenic mitigation efforts, such as controlling WWTP releases may have minimal impacts because current lake sediments were not statistically different from the sediment samples. By contrast, Randall et al. (2019) concluded that lake eutrophication may be reflected in phosphorus in sediments deposited near WWTP outfall locations. Williams et al. (2023) noted that discernable increases in nutrients and metals can be seen after pioneer settlement in the analysis of multiple sediment cores from UTL. Most recently, Taggart et al. (2025) performed a thorough geochemical analysis on 10 lake sediment cores and concurred that there are visible anthropogenic effects on the sediment. This thesis adds to the previous research and interpretation with three additional sediment freeze cores. More importantly, it evaluates the mechanisms and magnitudes of P release to the lake's water column from internal cycling by analyzing the porewater geochemistry with depth.

2.2 METHODS

2.2.1 Sediment Collection and Core Processing

Freeze cores reduce the disturbance of unconsolidated water-saturated lake sediments during sampling, leaving both porosity and sediment porewater undisturbed. Two freeze cores were taken from UTL in November 2024 and then in May 2025 following the methods of Williams et al. (2023). The 2024 and 2025 cores were taken at a location near that studied by Williams et al. (2023), west of Utah Lake State Park near the seasonally placed Utah Division of Water Quality buoy (UTL24-DW and UTL25-DW) (Figure 3). This represented a deep-water

location where a 20 cm sediment core was retrieved in 2024 and a 50 cm sediment core in 2025 in 3.9 m of water. The second freeze core location was near the Lindon Marina and Timpanogos Special Service District (UTL24-TSSD), representing a shallower-water location where a 35 cm sediment core approximately 2.3 m below water surface was obtained.

After collection, each core was vacuumed sealed, kept frozen at -25°C, and processed within 2 weeks of collection to minimize porewater sublimation. Cores were cut and measured following Williams et al. (2023). The 2024 cores were cut approximately 1 x 1 x 7 cm, for each cm depth, whereas 2025 decreased the depth resolution to every 2 cm depth. This experiment required each depth to be cut into two subsample cuboids: one for porewater chemistry and one for stable oxygen and hydrogen isotopes.

2.2.2 Porewater Stable Isotopes

A cuboid was placed in a centrifuge tube and allowed to melt with the lid tightly closed to prevent evaporation. The tubes were spun at 12,100 rpm to extract the porewater from each sample by causing the sediment to compact and expel porewater. Using an LGR -Model LWIA-24d – Liquid Water Isotope Analyzer, oxygen ($\delta^{18}O$) and hydrogen (δD) stable isotopes were measured for each water sample. The results were normalized relative to the VSMOW standard. Analytical precision of all samples ranged from ±0.2 for $\delta^{18}O_{VSMOW}$ and ±1 for δD_{VSMOW}.

2.2.3 Core Geochemistry

After careful dimension measurements, the second cuboid was placed in a pre-weighed centrifuge tube and weighed. To the 2024 DW and TSSD samples, 20 mL of ultrapure Milli-Q water were added to each tube and shaken for 24 hours and centrifuged. The 2025 samples only underwent ultracentrifugation at 12,100 rpm which compacted the sediment and allowed the

porewater to be decanted, filtered, and prepared with a 1:10 dilution for ICP and IC analysis. The remaining sediment was allowed to dry and then reweighed to calculate water loss and thereby determine dilution factors and porosities. Porosity was estimated by subtracting the mass of the water removed (1 cm^3 = 1 g) from the measured cuboid volume.

Residual dry sediment was lightly crushed with a mortar and pestle and analyzed by nitric acid digestion following the same methods from Williams et al. (2023) for 2024 samples. EPA Method 3051A was used for the 2025 samples (Taggart et al., 2025). At the time of Williams et al.'s work (2023), microwave digestion was not accessible but both microwave and manual methods used a high-temperature digestion, with aggressive acid in nonreactive screw cap Teflon beakers. Differences in results between the two methods are considered negligible (Chen and Q, 1998). After centrifugation, a 1:10 dilution of the acid digestion was made for each sample for ICP analysis. As a result, both porewater and sedimentary phosphorus and other trace metals were determined.

2.2.4 Phosphorus Fluxes

Although porewater anion analysis did provide orthophosphate results, the dilutions needed for the extractions produced data too close to instrument calibration limit for most subsamples. Instead, total phosphorus measurements were made by ICP-OES and then estimated orthophosphate concentrations using the geochemical modeling code PHREEQCi (Charleton et al., 1997).

Following the methodology of Fisher and Reddy (2013; Fick's first law) and the diffusion coefficient for orthophosphate from Li and Gregory (1974), diffusive fluxes were calculated as follows:

- Total phosphorus was converted from mg/L to mmol/L to estimate the maximum concentration of orthophosphate.
- Using estimations from PHREEQCi, the fraction of orthophosphate of the mean porewater in the gradient at a pH of 8 came out to be 57.2%. Based on molecular weights, phosphorus is 32.2 % of the orthophosphate ion.
- Orthophosphate in mmol/L was then estimated from these fractions.
- Orthophosphate was recalculated in mg/L.
- The diffusive flux (mass/unit area/unit time) was then multiplied by an assumptive constant surface area of Utah Lake (380 km^2) to obtain an annual flux.
- Fluxes are then reported as P in orthophosphate.

The expression for diffusive flux is given as:

$$(1)\ J = \phi \frac{D}{\theta^2} \frac{\partial C}{\partial z}$$

$$\phi = porosity$$

$$D = diffusion\ coefficient\ for\ orthophosphate = 5.22343 \times 10^{-6} cm^2 s^{-1}\ at\ 10.8\ ℃ \text{ (derived from Li and Gregory (1974)).}$$

$$\theta^2 = tortuosity = 1 - 2\ln(\phi)$$

$$\frac{\partial C}{\partial z} = the\ diffusive\ graident\ at\ the\ top\ of\ the\ core$$

For $\frac{\partial C}{\partial z}$, discretion was exercised on how much of the upper portion of the core is included in the linear regression. More analysis and research needed to be done to determine what has caused the disruption and lower gradients, so the top gradient and porosities were used since they exhibited what was happening in the lake at that point in time. The average porosity was calculated for the same interval.

2.3 RESULTS AND DISCUSSION- Freeze Core Analysis

2.3.1 Porewater Stable Isotopes

Stable isotope (δD / $\delta^{18}O$) analysis on the core porewater allowed investigation of the vertical movement of water through lake sediment. Standards and samples were corrected to VSMOW and plotted with the UTL local evaporative line (LEL) (Figure 9a) (Zanazzi et al., 2020). All porewater samples plotted slightly below the LEL.

The δD and $\delta^{18}O$ isotopic variation of the UTL24-DW samples was minimal as a function of depth (Figure 9b). Alternatively, δD and $\delta^{18}O$ UTL24-TSSD samples showed a clear linear correlation of increasingly depleted isotope ratios with depth. UTL25-DW samples plotted between the two samples also with a significant correlation with depth.

These results suggest that UTL24-TSSD and UTL25-DW indicate mixing between groundwater and evaporated lake. To illustrate this, a mixing line was created to demonstrate the influence of groundwater in the samples (Figure 10). The lake water endpoint was set utilizing the δD and $\delta^{18}O$ from the sediment water interface sample and the groundwater endpoint was set averaging δD and $\delta^{18}O$ data from 3 near offshore groundwater samples: Vineyard Main Street (40.2995278, -111.7528889), northeast of Lindon Marina (40.3438056, -111.7481944), and a nearby canal that leads to Powell Slough (40.272983, -111.729445) (Waterisotopes Database). The calculated groundwater influence was averaged at 28% for UTL24-TSSD and 13% for UTL25-DW.

The lack of correlation in oxygen and hydrogen isotopes with depth in UTL24-DW likely represents a lack of mixing at the site of this core on the date it was sampled. However, the clear mixing with an isotopically depleted endmember for the other two cores, probably groundwater,

was most likely due to upwelling groundwater. This implies that there is upward seepage through the fine-grained marl sediment on the lake bottom. In turn, the diffusive fluxes of phosphorus discussed next are affected by an advective term, the magnitude of which remains to be determined.

2.3.2 Porewater Geochemistry

Major and trace elemental analysis provided geochemical insight into the diffusive and advective release of phosphorus into the water column in the three core samples (Figure 11). The UTL24-DW core shows a gradual diffusive trend in phosphorus (i.e., negative slope) from out of the sediment into the overlying water column, whereas UTL24-TSSD and UTL25-DW show an overall positive sloping gradient interrupted by breaks with steep negative gradients near the top. It is possible these breaks could be indicative of horizons of organic rich material, but more research is needed to investigate the organic vs nonorganic phosphorus at these intervals. The near-surface negative trends are concluded to reflect diffusive loss of phosphorus, possibly augmented by advection. There is a large potential gradient between lake water (mean=70 µg/L; Williams et al., 2020) and the much larger porewater concentrations of phosphorus.

The groundwater mixing evidence seen in the stable isotope suggests that phosphorus levels in UTL24-TSSD and UTL25-DW are influenced as seen with concentrations decreasing near the base of the cores because of upward fluid movement. Even though the DW cores were taken at a relatively similar location (Figure 3), contrasting phosphorus profiles could be due to the fact they are taken at different times of year (fall 2024 vs spring 2025) when ground water influence varied, although 2024 was only 20 cm and may not have captured this effect. Another factor that could lead to differences in the DW cores is variability in local hydro-stratigraphy. Like on land, springs or notable groundwater influence may only occur at discrete points or

restricted areas. Even though UTL24-TSSD was also taken in fall 2024, due to the shallower nature of the sampling location, significant groundwater influence is assumed to take place year-round.

The decreasing phosphorus gradients within the UTL24-TSSD and UTL25-DW core could be due to more oxic conditions occurring near the surface, resulting in the sorption of phosphorus on iron-oxides (Ding et al., 2016). This can be further supported by utilizing the anion results. Firstly, the assumption was made that a decrease in porewater sulfate was indicative of oxic/ anoxic conditions because of sulfate reducing bacteria rather than groundwater mixing due to the depth of occurrence (Berg et al., 2025, Heinrich et al., 2021, Komor, 1992). Correlating the sulfate along with trace metals of iron, manganese, and phosphorus with depth reveals UTL24-DW did not enter anoxic conditions in the sampled 20 cm while UTL24-TSSD exhibits a clearer oxidation-reduction process. UTL24-TSSD shows sulfate reduction is active and manganese/ iron are being reduced around 20 cm (Figure 12). Iron and manganese in UTL25-DW do not show an increase with depth like the UTL24-TSSD core. In the UTL24-TSSD core, porewater was extracted by adding Milli-Q water, which may have liberated lightly sorbed metals, whereas in UTL25-DW, porewater was extracted by compaction during centrifugation such that there was no tendency for desorption. UTL25-DW has a lower decrease in sulfate and even at 50 cm may not have reached minimum values. This could indicate incomplete reduction or possibly transitional scenario.

2.3.3 Estimated phosphorus diffusion from porewater geochemistry

After using Fick's first law of diffusion (Fisher and Reddy, 2013) an average of the three cores provided first estimates of internal phosphorus cycling (Figure 13a). Using the Arrhenius equation, which helps us understand how temperature affects the speed of a chemical reaction,

core diffusion estimates were calculated monthly for phosphorus contribution (Figure 13b). UTL24-DW had the highest total phosphorus contribution (6.97 mg P m^{-2} d^{-1}) while UTL24-TSSD and UTL25-DW were similar (4.94 mg P m^{-2} d^{-1} and 5.17 mg P m^{-2} d^{-1}, respectively). For easier comparison to other UTL estimates, these numbers were corrected to an area of 380 km^2 where respectively the phosphorus contribution was 967 mT/yr, 685 mT/yr, and 717 mT/yr. The phosphorus fluxes presented could be maximum in the case of the UTL24-DW due to little ground water influence in the fall or a minimum due to the flushing of ground water in the spring as shown in UTL25-DW.

The average of the three cores was compared to the other phosphorus sources to the lake (Figure 13c). In the most recent conclusive study, Barrus et al. (2021) determined that AD contributed between 133 and 262 mT/yr to UTL. The higher range was not screened, allowing total P to be collected, while the lower range exhibited a 50% decrease after screens were implemented to reduce insects. Since insects landing in the samplers were not the source of extra phosphorus (S. Nelson, personal communication, December 2024), the screens likely reduced the ability to collect dust. For this comparison, the 262 mT/yr was used and represented 22.5% of the pie chart. Forecasts of WWTP upgrades to 1 mg/L TP at the seven surrounding plants estimate an annual P load of 71 mT/ yr. When all the WWTP upgrades are complete, under current flows and standard biological phosphorus reduction, the average annual load from wastewater facilities will be less than 60 mT/yr which accounts for 5.2% of the pie chart (L. Myers, personal communication, December 2025). Since this is the only loading term readily impacted by engineering controls, and studies suggest that European settlement has increased dust in the western US by 500%, AD is beyond WWTP control and represents an anthropogenic source (Neff et al., 2008). Finally, about 4.3% is from streams based on the UTL Science Panel estimate

of TP contribution from tributaries and nonpoint sources to the lake (50 mT/yr, T. Miller, personal communication, December 2025). Assuming the average sediment flux is accurately calculated, 68% of phosphorus added to UTL water comes from porewater (790 mT/yr).

For perspective, comparison was made to Orihel et al.'s (2017) database which provided 369 gross flux estimates of internal P loading from 70 Canadian freshwater locations (Figure 14). They found that the median gross benthic phosphorus flux retrieved through sediment incubation experiments for a eutrophic lake was 6.9 mg TP m^{-2} day^{-1} which normalized to the area of UTL (380 km^2) is about 957 mT-P/year. UTL freeze core samples also fell into the high category based on OECD (Organization for Economic Co-operation and Development) standards for phosphorus assessment, which provide standardized protocols for measuring nutrients, evaluating water quality, and reporting pollution. Although the OECD does not provide specific numeric classifications for phosphorus fluxes from sediments, its nutrient load and eutrophication frameworks offer a benchmark for assessing the relative significance of sediment-derived phosphorus.

More research will clarify the variation in the contribution of diffusion and advection across the lake, but it is safe to assume that phosphorus from UTL sediment porewater is a significant source and management strategies targeting this source would exert a greater influence on lake health than just reducing WWTP releases. One suggested option would be to help recultivate the periphyton layer so that constituents entering the water column from the sediment might be taken up at the lake bottom (King et al., 2023). Productivity in the periphyton would decrease planktic algal productivity and therefore improve water clarity and decrease algal blooms. A reestablished periphyton would also increase the stability of bottom sediment. This might involve reducing or eradicating carp and reestablishing emergent vegetation to realize

improved water clarity. This is important for enabling the visual predation of juvenile carp by other fish species (Richards & Miller, 2022).

2.3.4 Sediment Geochemistry

William et al. (2023) collected three UTL cores in August 2019 and analyzed the sediment via acid digestions to observe phosphorus and other trace elements in the lake sediment from Goshen Bay, Provo Bay and one from approximately the same location as the DW cores. Research has shown that the two UTL bays are geochemically different from the main body, so only the Williams DW core is compared here. This research adds to that previous data and shows that while cores were taken in a relatively similar location, each core is different due to water conditions and seasonality. As mentioned previously, sediment sample showed the results of the availability of loosely bound iron due to the MilliQ porewater extraction in UTL24-DW and UTL24-TSSD (Figure 15a).

2.3.4.1 Sediment Phosphorus

Phosphorus seemed to be unaffected by the different porewater extraction methods and research has shown that lightly bound phosphorus makes up less than 3% of the total phosphorus-fraction percent in UTL sediment (Jarvis, 2023, LeMonte et al., 2023). The four cores ranged from 453 to 1044 mg/kg total phosphorus with UTL24-TSSD having the lowest numbers and Williams DW having the highest (Figure 15b). The average total phosphorus was ~745 mg/kg which is similar to Williams et al. (2023) DW and UTL25-DW cores averages. Comparatively, Taggart et al.'s (2025) 10 sediment cores ranged from 166 to 941 mg/ kg with an average of 530 mg/kg. This lower average could be a result of differing methodology including

only taking samples near shore, greater analyzed depth (140 cm) that captured phosphorus stabilization, seasonality (summer 2024), or an open-barrel core collection method.

Based on ^{210}Pb and ^{137}Cs chronologies, Williams et al. (2023) hypothesized that the rise of phosphorus concentrations in the cores came from the increased phosphorus loading from the anthropogenic influenced discharge of the surrounding growing population in the early 1900s especially seen in Provo and Goshen bays. For the Williams DW core, ^{210}Pb dating was inconclusive so changes in pollen established the timing of European settlement. A similarity was seen in the UTL24-TSSD core at about that depth with UTL25-DW showing increases in trace metals and phosphorus starting a little deeper (26 cm).

For comparison, this study also performed acid digestion on UTL suspended sediment samples taken near Bird Island at the time of filter collections. Although not specifically reported in this thesis, X-ray diffraction results for the suspended sediment are preserved in an appendix located at the end of the thesis. Nine samples were processed ranging from July 2024 to November 2024. Phosphorus concentrations exhibited substantial variability, ranging from 807 to 3239 mg/kg—representing approximately a four-fold difference—with a mean of 1310 mg/kg over the period. This shows that the average suspended sediment that settles on the bottom of the lake contains almost twice the amount of phosphorus that is seen in the lake sediment. This excess phosphorus likely originated from organic matter that rapidly decomposes and releases phosphorus to the pore water, thereby accounting for the much higher concentrations of this element in pore compared to lake water.

2.3.4.2 Sediment Trace Metals

Williams et al. (2023) thoroughly analyzed lead (Pb), copper (Cu), and zinc (Zn) in cores to examine the anthropogenic effects of surrounding industrial activities. For context, the primary adjacent shore industrial site is the Geneva Steel site. The plant was completed in 1944 to support the World War II effort and closed by 2001 due to company bankruptcy (GPM Enviro Project Manager, LLC, 2025). Being so close to the plant, various constituents were discharged into UTL. A report by the Environmental Working Group found that just from 1990 to 1994, Geneva Steel released a total of 266,468 pounds of toxic pollutants into Utah Lake (Savitz et al., 1996). Previous beliefs were that the lake was self-cleansing due to mixing, but further remediation remains necessary (Bishop et al., 2024).

Similar trace metal patterns were observed between 25-DW and Williams DW, but the short depth of UTL24-DW did not allow for adequate comparison (Figure 15b). TSSD, which is shore adjacent to the Geneva Steel site as well as WWTP output, showed a similar increasing pattern to the other cores. By correlating this core to Williams et al. (2023) DW, the increases seen at 20 cm are believed to be around the early 1900's. Anomalous spikes in lead and zinc at about 16 cm depth may be due to the opening of Geneva Steel or the other waste that was discharged into the lake until 1967 when state law began to prohibit raw sewage (Bishop et al., 2024). This could be evidence of anthropogenic effects but also aligns with the porewater marker for that core where iron and sulfate decrease due to reducing conditions. While the upper sediments may be subject to mixing, the preserved trace metal patterns indicate that deep mixing is not occurring.

2.4 CONCLUSIONS

- Comparison of stable isotopes (δD and $\delta^{18}O$) in pore water with depth indicate the variation of groundwater influence at various locations and season in the lake, influencing upward diffusion and advection from pore into lake water.
- Potential redox indicators, including using sulfate, iron, and manganese are observed, which influence the phosphorus concentrations through adsorption/desorption reactions.
- Using the diffusive phosphorus gradients from cores, estimates of phosphorus fluxes were made indicating up to 70% of the phosphorus input into UTL is from sedimentary pore water. Potential reactive phosphorus (OP) from the sediment still holds almost a third of the phosphorus input showing that changes at wastewater treatment plants would provide minimal effects on the overall phosphorus loading.
- The phosphorus seen in the solid sediment is significantly lower than the suspended sediment that eventually settles on the lake bottom, suggesting that a significant fraction of sedimentary phosphorus is rapidly released to porewater, consistent with porewater concentrations that are much higher than the water column.
- Sediment trace metals in the new cores are consistent with previous cores studies (i.e. Williams et al., 2023, Taggart et al., 2025), indicative of anthropogenic effects recorded in lake sediment as well as redox effects. Overall, there is a transition from oxic to anoxic conditions over the upper 20 cm of sediment.

FIGURES

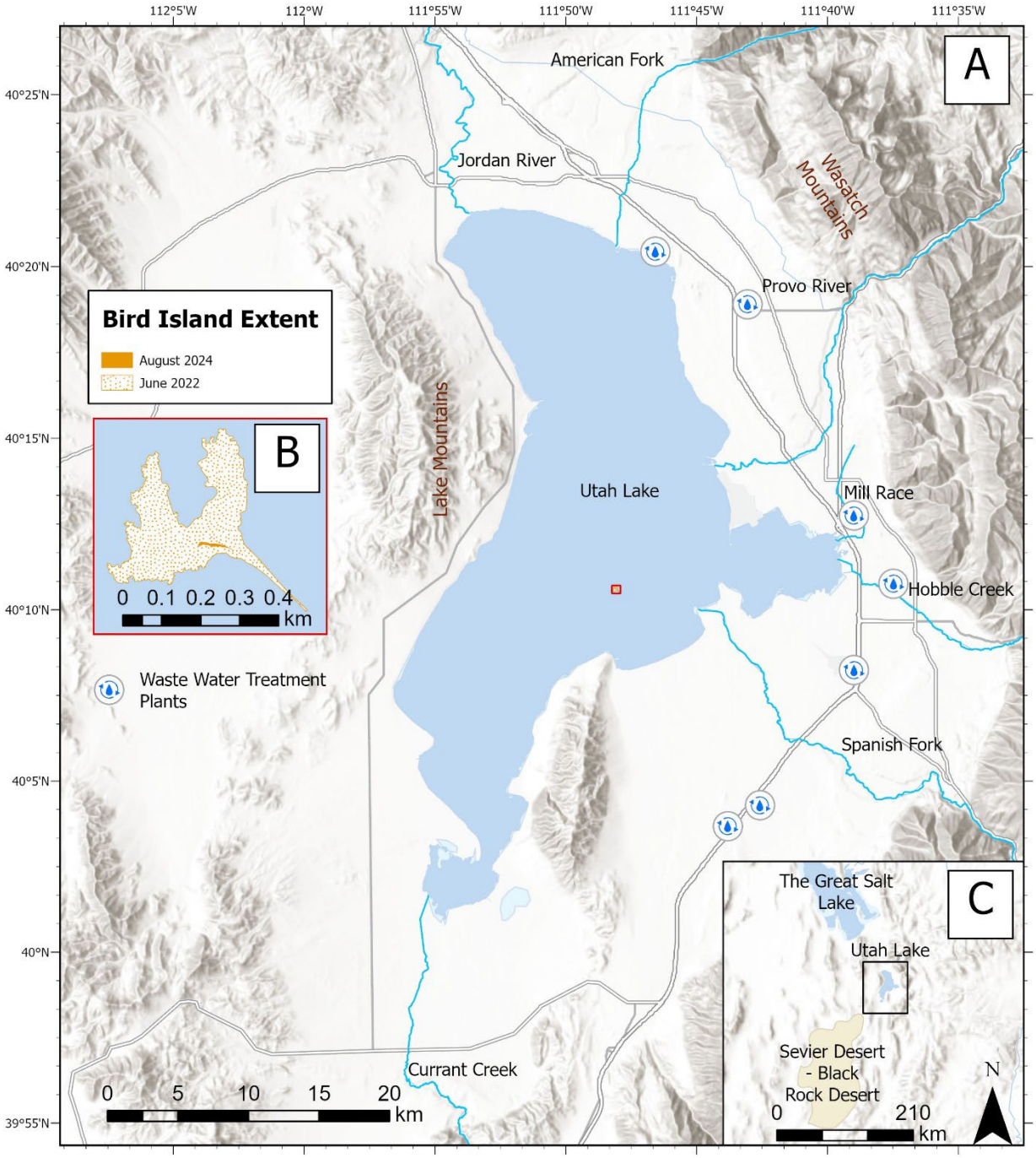

Figure 1: A) This map shows Utah Lake (UTL), located approximately 60 km sourth of Salt Lake City, UT. UTL is the center of a heavily poulated part of Utah Count and contains one small island, Bird Island. Because lake levels change depending on precipitation, Bird Island size is extremely variable. B) This map shows the extent of Bird Island between two years. Fieldwork for this project was conducted during the 2024 water year.C) Map shows the relation of the Great Salt Lake, UTL, and the Sevier Desert-Black Rock Desert area where Seveir Lake used to reside.

Figure 1

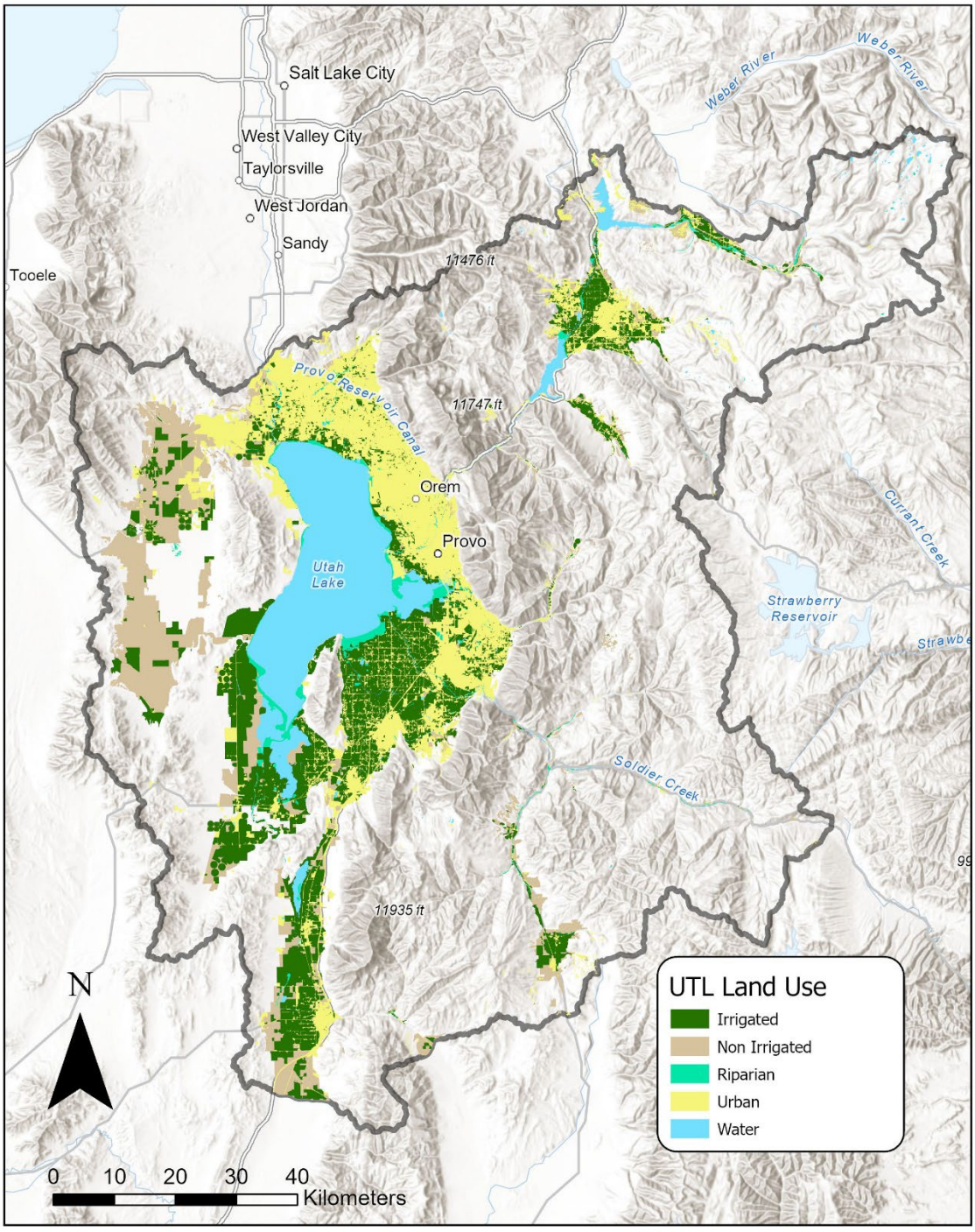

Figure 2: This map shows the Utah Lake Watershed with the surrounding land use differentiated. We see heavy irrigated agriculture as well as urban use which is a significant source of nutrients to the lake. Map adapted from Utah Lake Basin Planning for the Future Report (Utah Division of Water Resources, 2014).

Figure 2

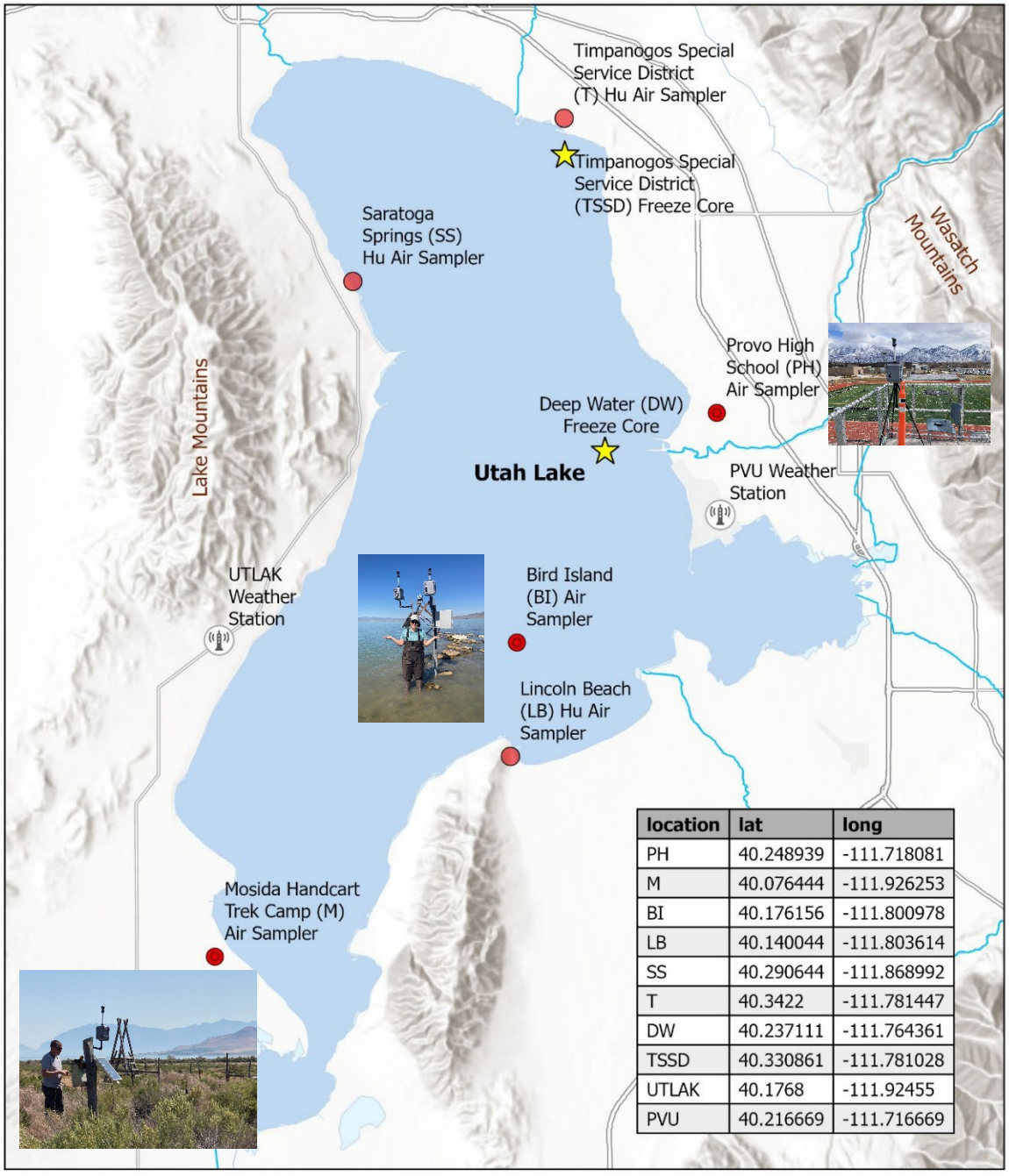

Figure 3: This map shows the locations of this research as well as the locations of data collected from Hu et al (2025) and local weather stations.

Figure 3

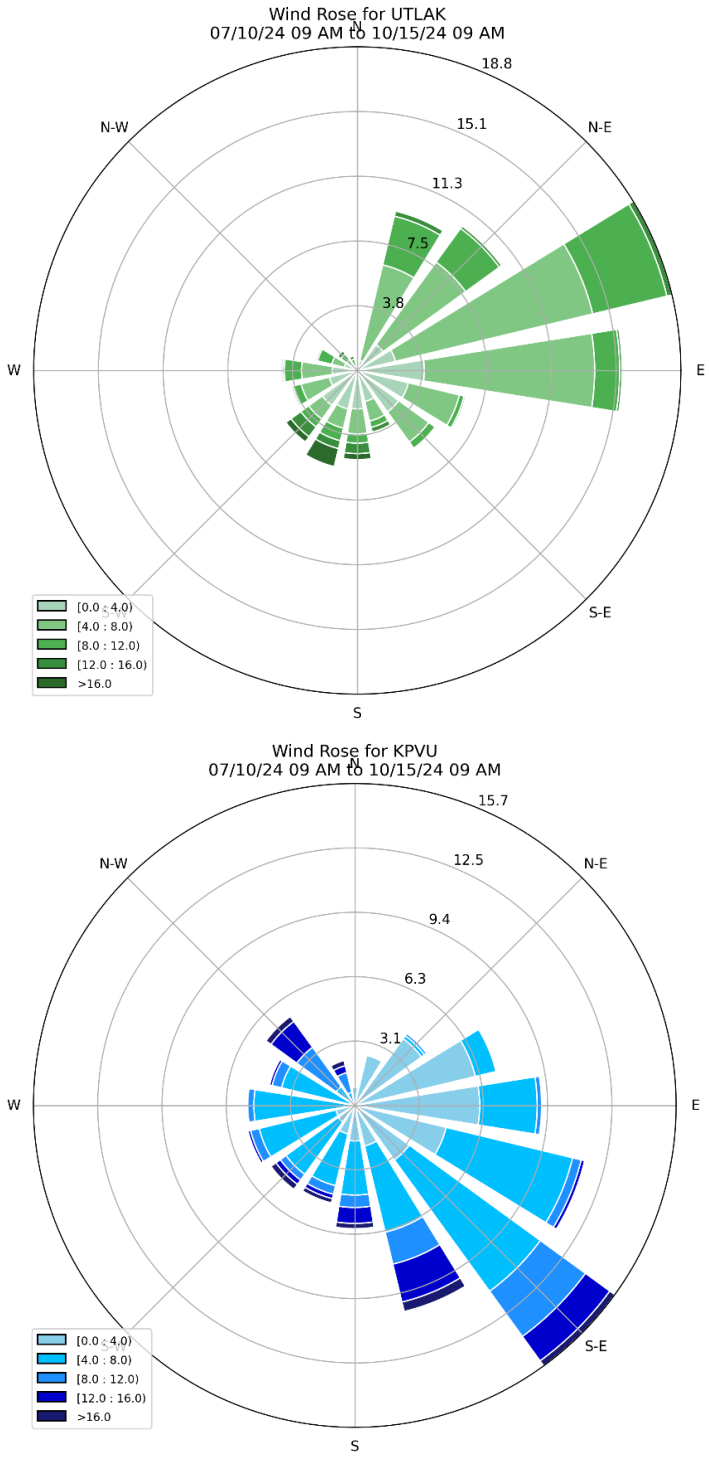

Figure 4

Wind direction Rose Diagrams from weather stations near the air samplers placed. Data was pulled for the collection period. On the western side of the lake, UTLAK shows a predominate northeast direction while on the eastern side of the lake, KPVU shows a predominant southeast direction.

a

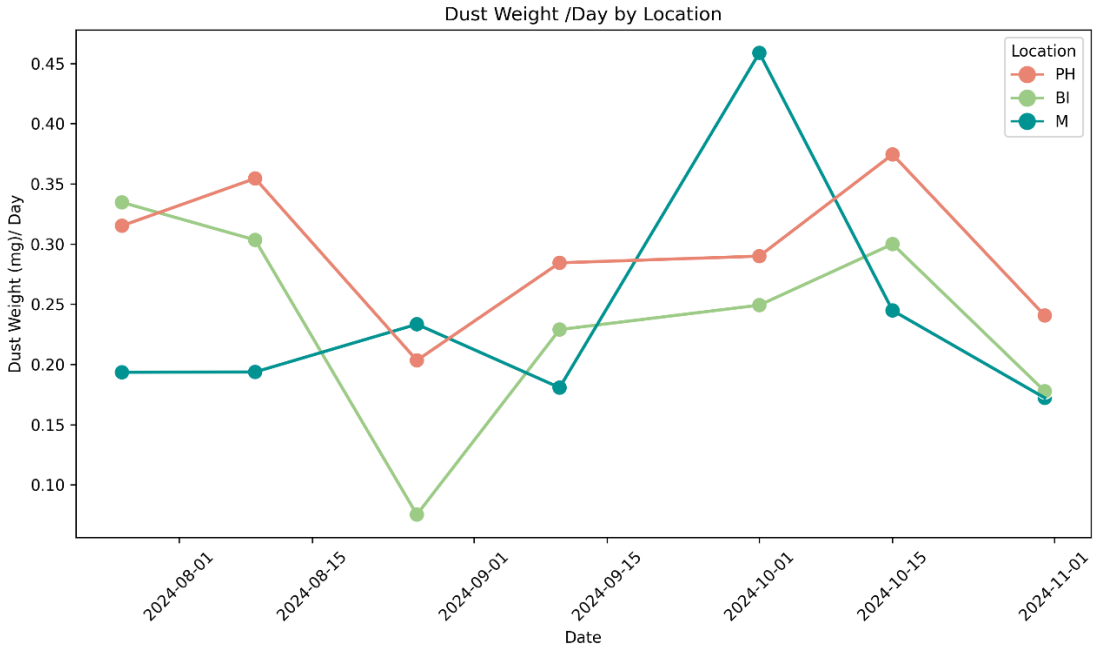

b

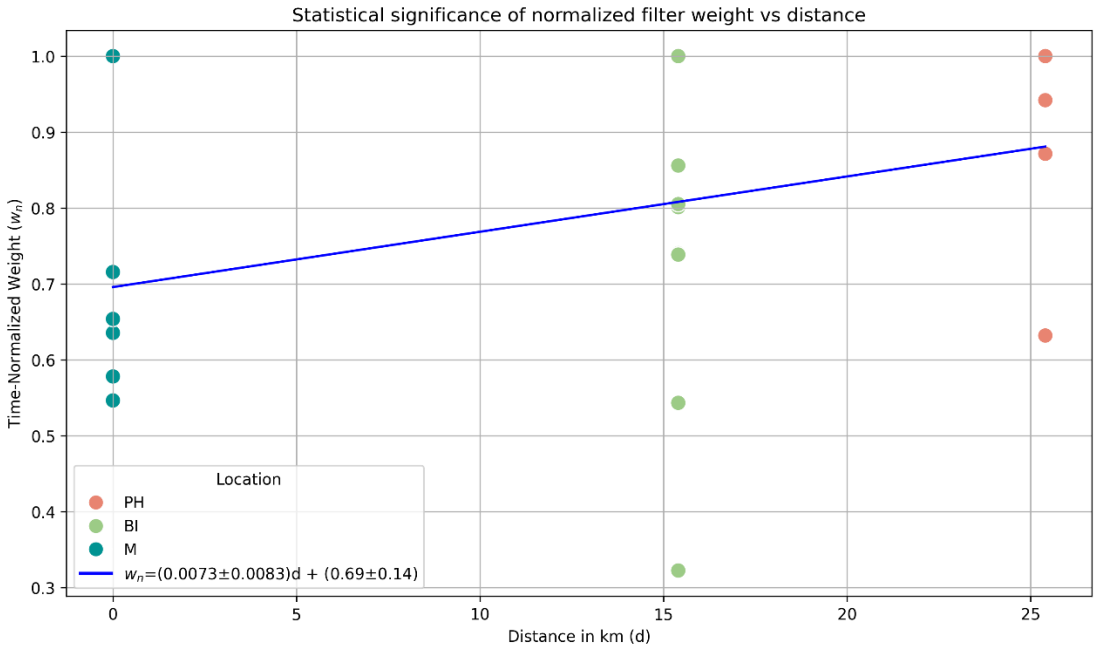

Figure 5

a) The dust weight accumulated per day over time for each sampling location. These are plotted based on filter collection date. To evaluate the statistical significance of the data, b) shows the previous data normalized and plotted against distance from Mosida (M) to Bird Island (BI) to Provo High (PH). The slope encompasses zero, indicating that there is no significant evidence of dust attenuation for this data.

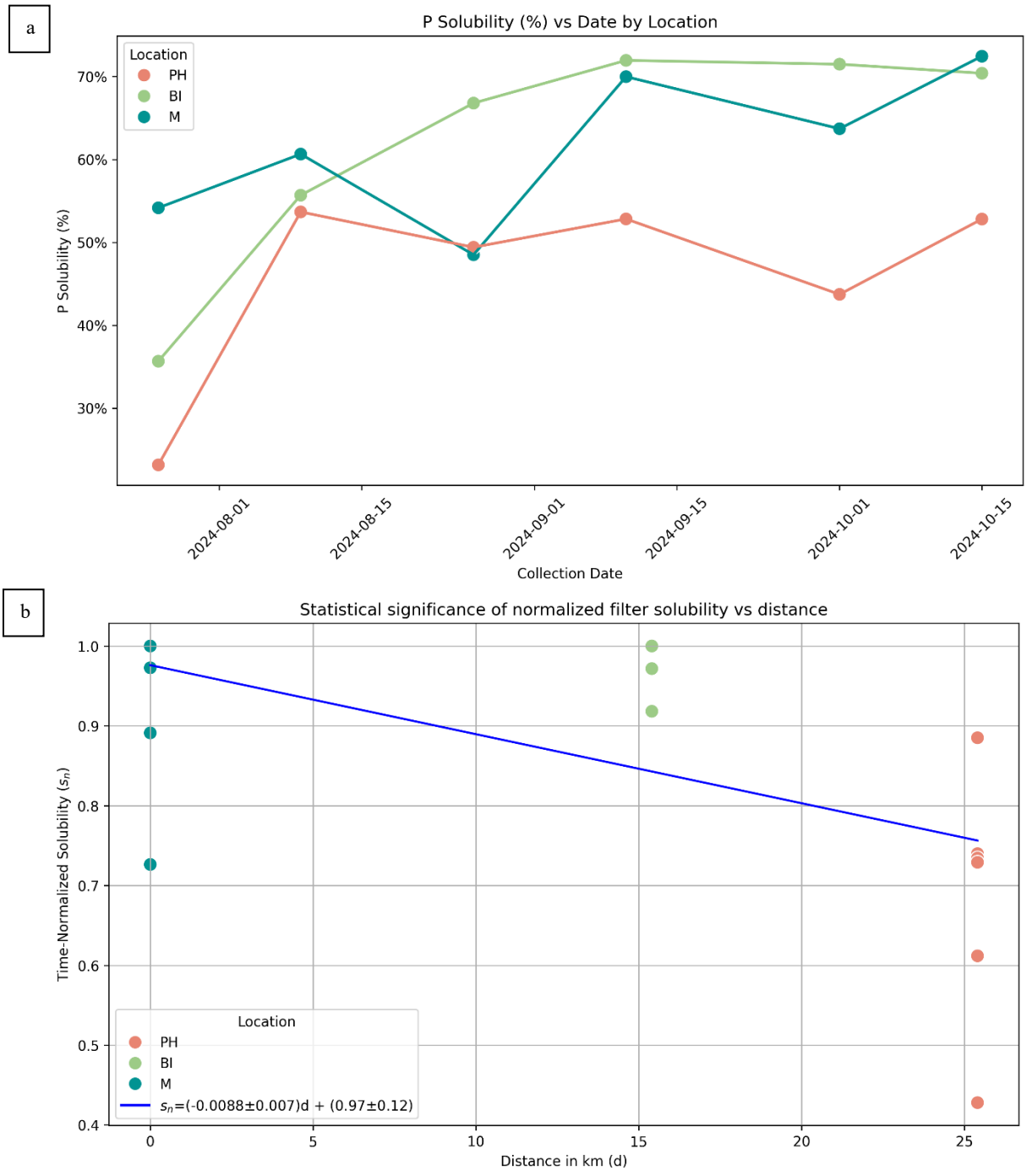

Figure 6

a) The phosphorus solubility in the filters over time for each sampling location. To evaluate the statistical significance of the data, b) shows the previous data normalized and plotted against distance from Mosida (M) to Bird Island (BI) to Provo High (PH). The slope does not encompass zero, indicating there is a significant decrease in solubility from the SW to NE direction across the lake.

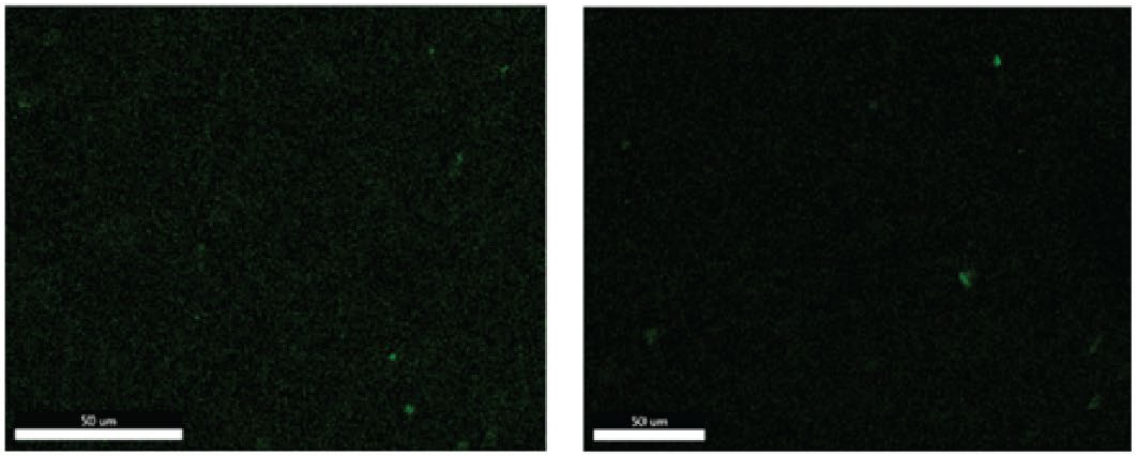

Figure 7a: Timpanogos 2023 (T 2023) filter showing two qualitative P maps. Bright green spots indicate P hotspots" This was a prelminary run and correlating elements was not available.

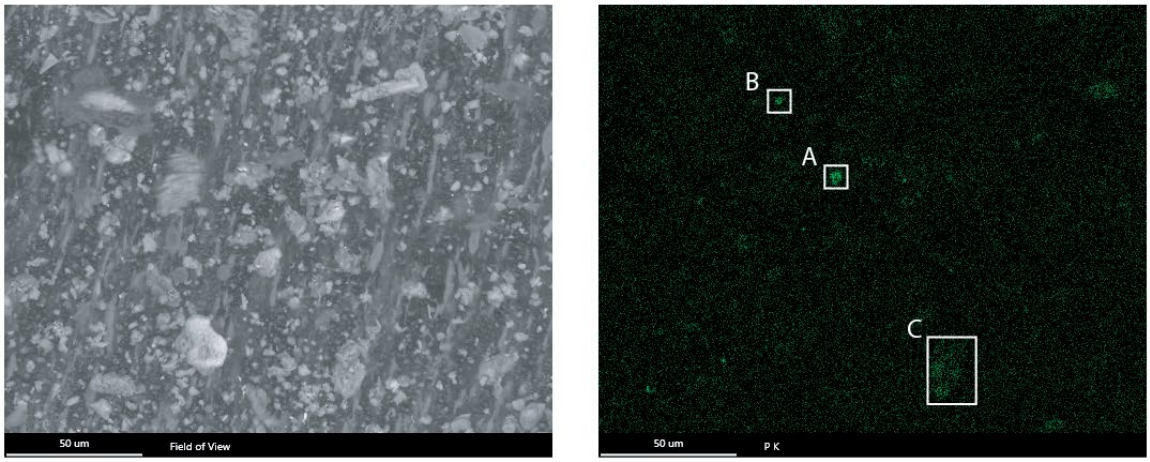

Figure 7b: Bird Island 2024 (BI 2024) filter showing field of view (left) and P elemental map (right). Boxes emphasize noted and studied hotspots but elemental correlation was inconclusive due to low resolution.

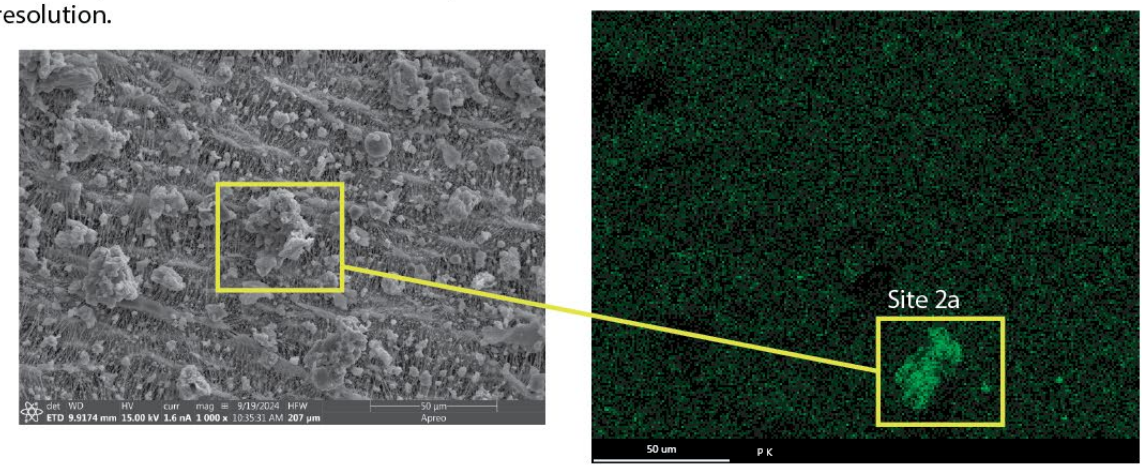

Figure 7c: Provo High 2023 (PH 2023) filter showing higher resolution electron scatter image (left) and P elemental map (right). This was the largest hotspot found in random scans and was picked for further elemental analysis.

Figure 7

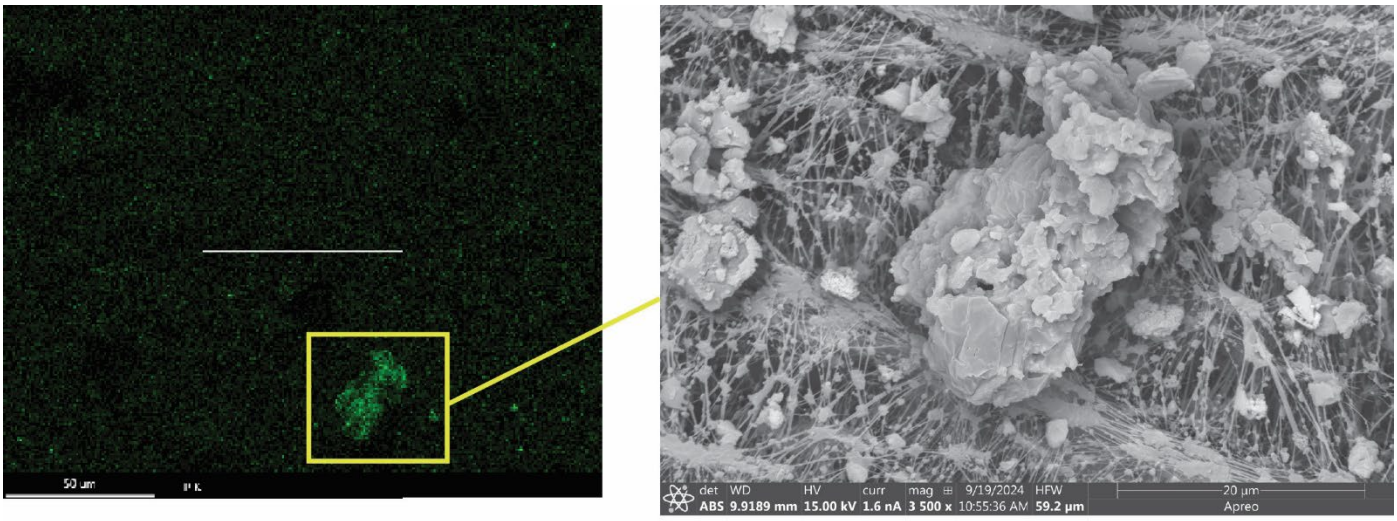

Figure 8a: Provo High 2023 (PH 2023) filter showing P elemental map (left) and zoomed in higher resolution electron scatter image to highlight the main P hotspot (right).

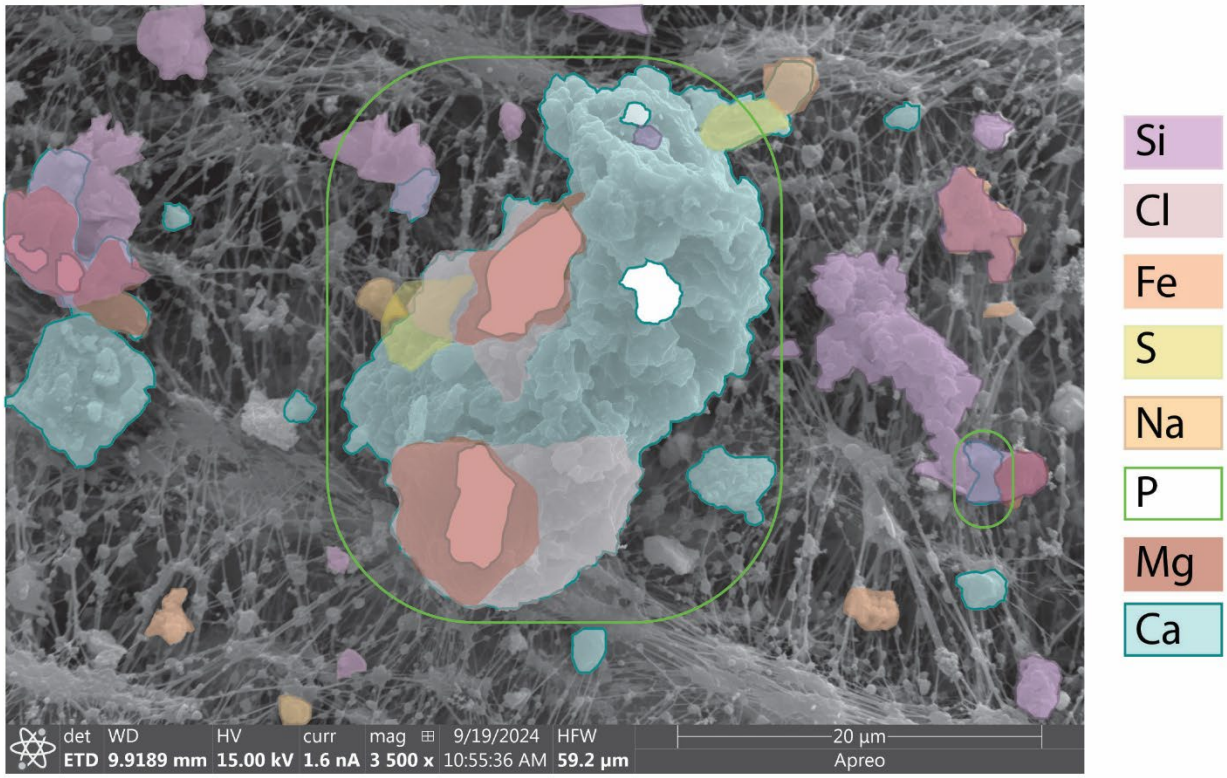

Figure 8b: Manual elemental overlay map tracing of the particle seen in site two of the Provo High 2023 (PH 2023) filter shows calcium correlation (blue) with the phosphorus hotspots (green).

Figure 8

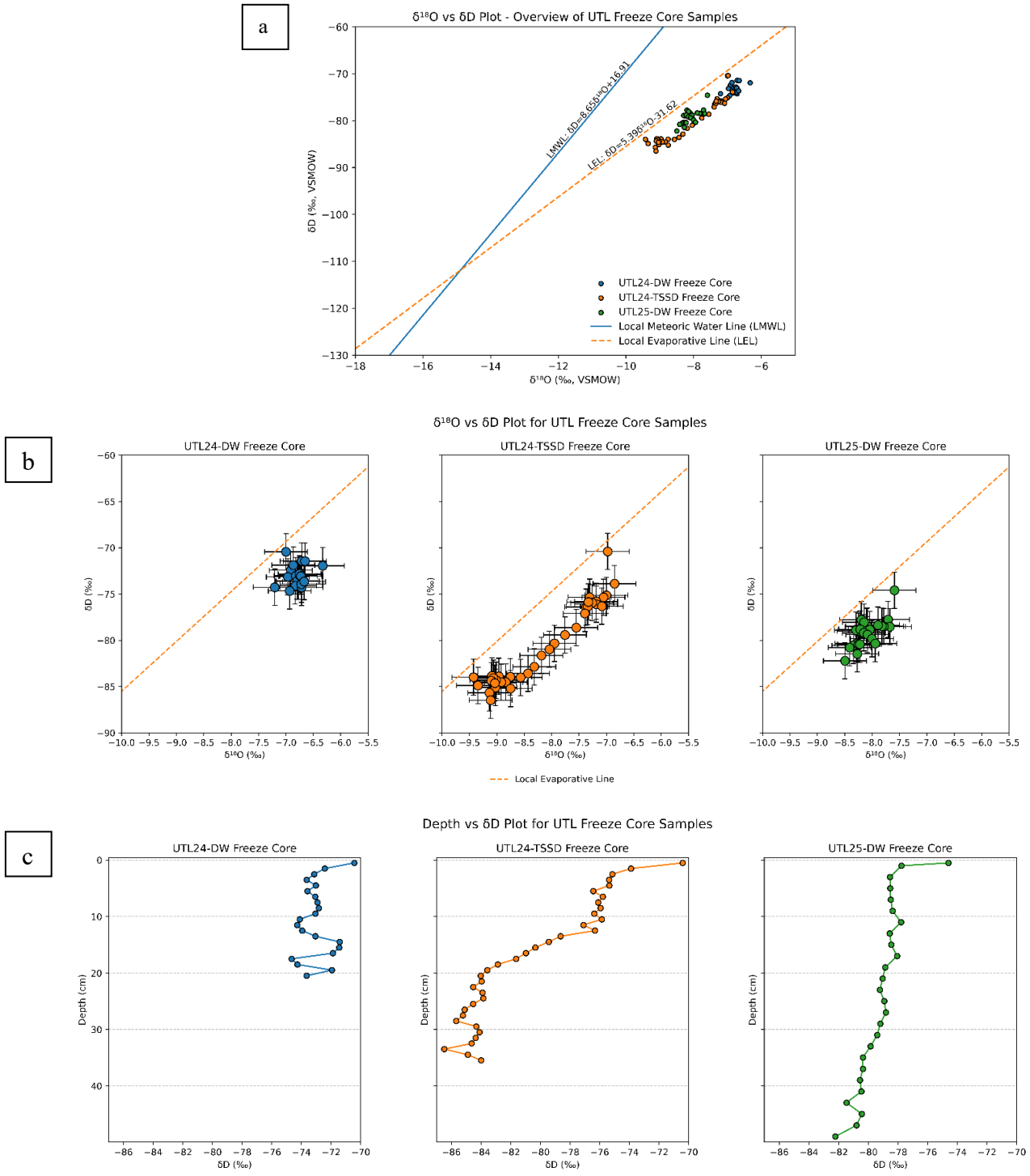

Figure 9

a) Graph shows an overview of the oxygen ($\delta^{18}O$) and hydrogen (δD) stable isotopes that was measured for each freeze core porewater sample. b) A zoomed in version shows the more specific patterns for each core: UTL24-DW clusters, UTL24-TSSD depletes with depth and UTL25-DW seems to be a mix of both. c) Graphs show changes in δD for each core with depth.

Groundwater Isotope Values

Site Name	Location Description	Coordinates	$\delta^{2}H$ (‰)	$\delta^{18}O$ (‰)
(D-6-2)17bcb-1	Vineyard Main St	40.29953, -111.75289	-121	-16.07
(D-5-2)32bdb-2	Lindon directly NE of marina	40.34381, -111.74819	-120	-16.24
Isotope Sample X	Canal that leads to Powell Slough	40.27298, -111.72944	-123.0355	-16.3733
Average			-122.8071	-16.42866

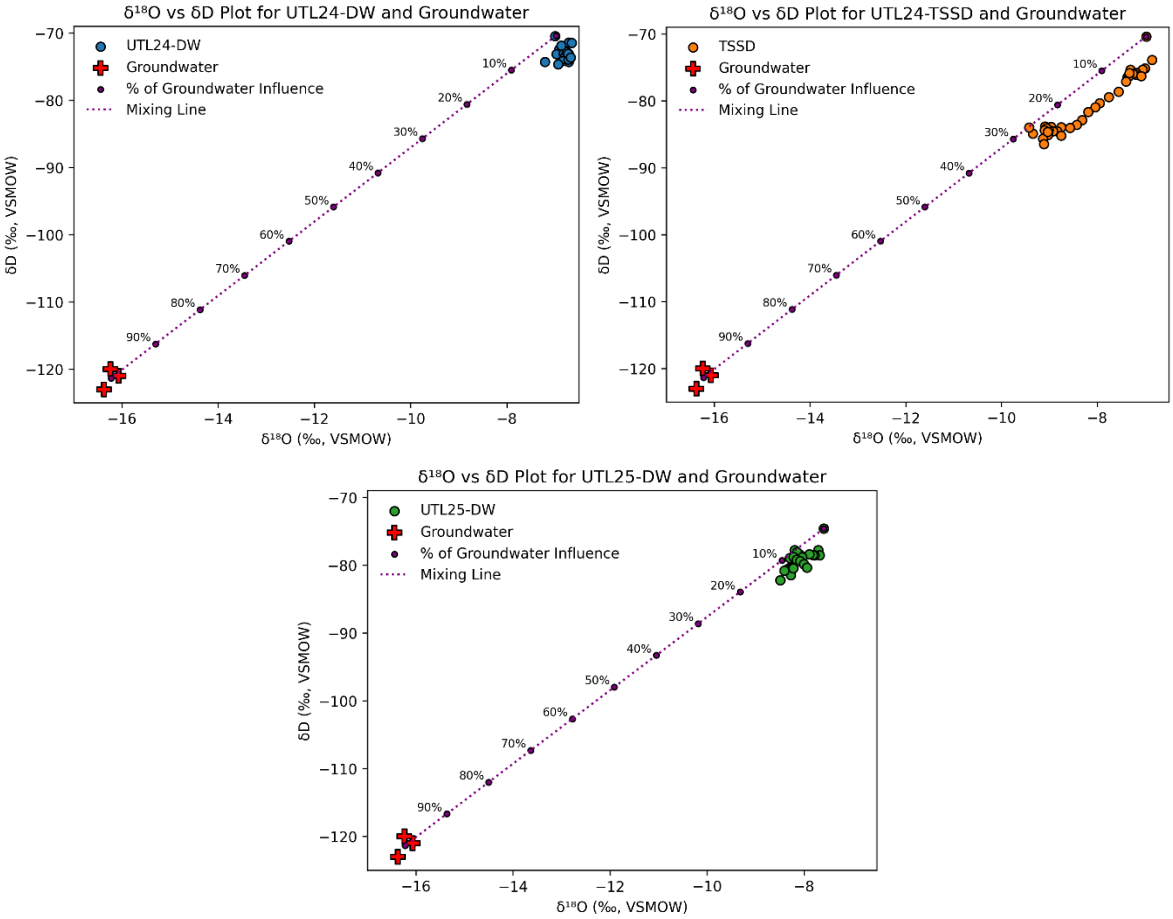

Figure 10

Mixing lines were created based on an average of local, offshore groundwater isotope samples (table) (Waterisotopes Database). Graphs show evidence of groundwater mixing with depth for UTL24-TSSD and UTL25-DW while UTL24-DW is plotting near lake water conditions.

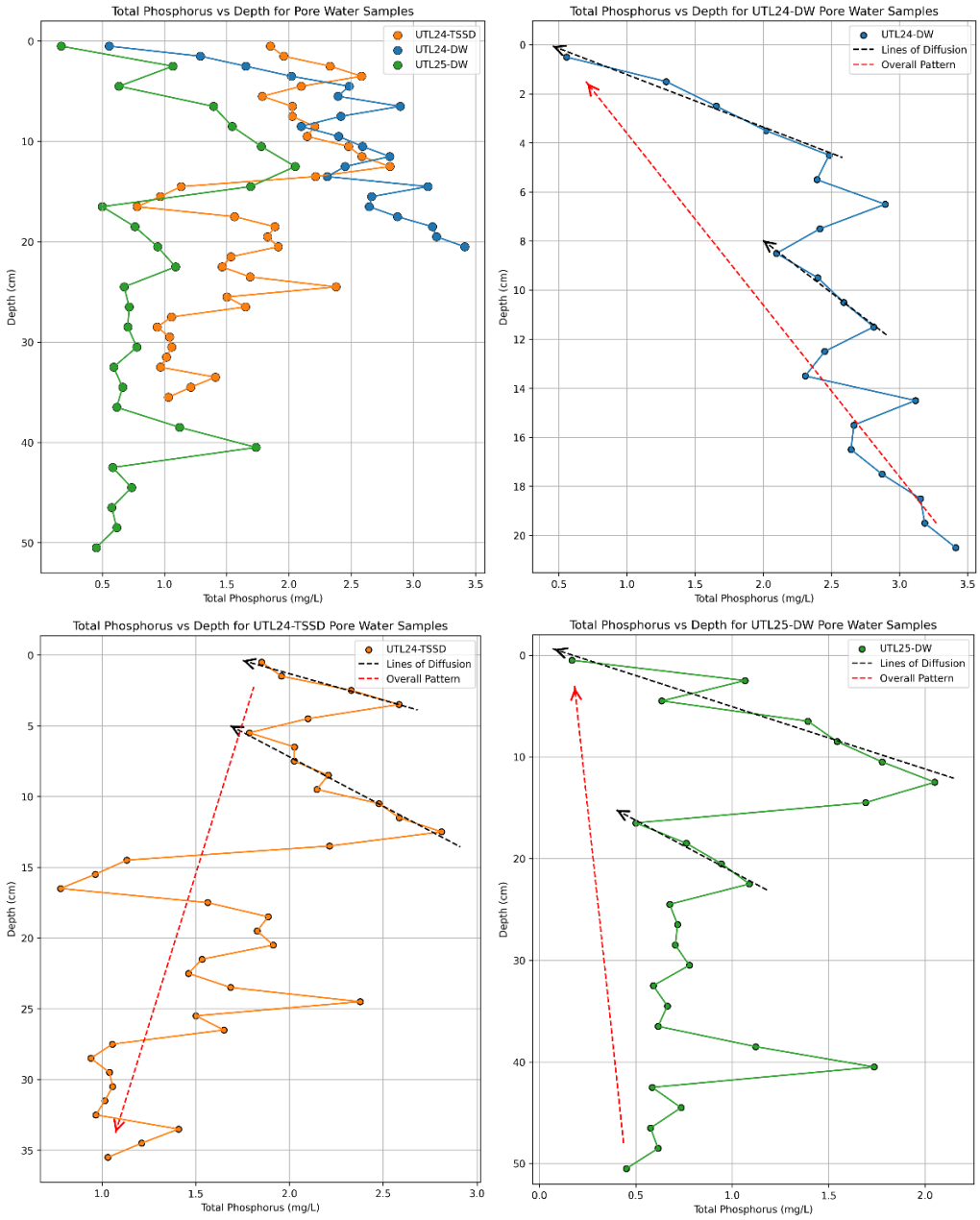

Figure 11

Total phosphorus in porewater vs depth for each of the three freeze cores. Note the different scales for each core. Each show diffusive gradients at the top, but the UTL24-TSSD and UTL25-DW level out at the bottom of the cores, possibly indicating advection due to groundwater flushing.

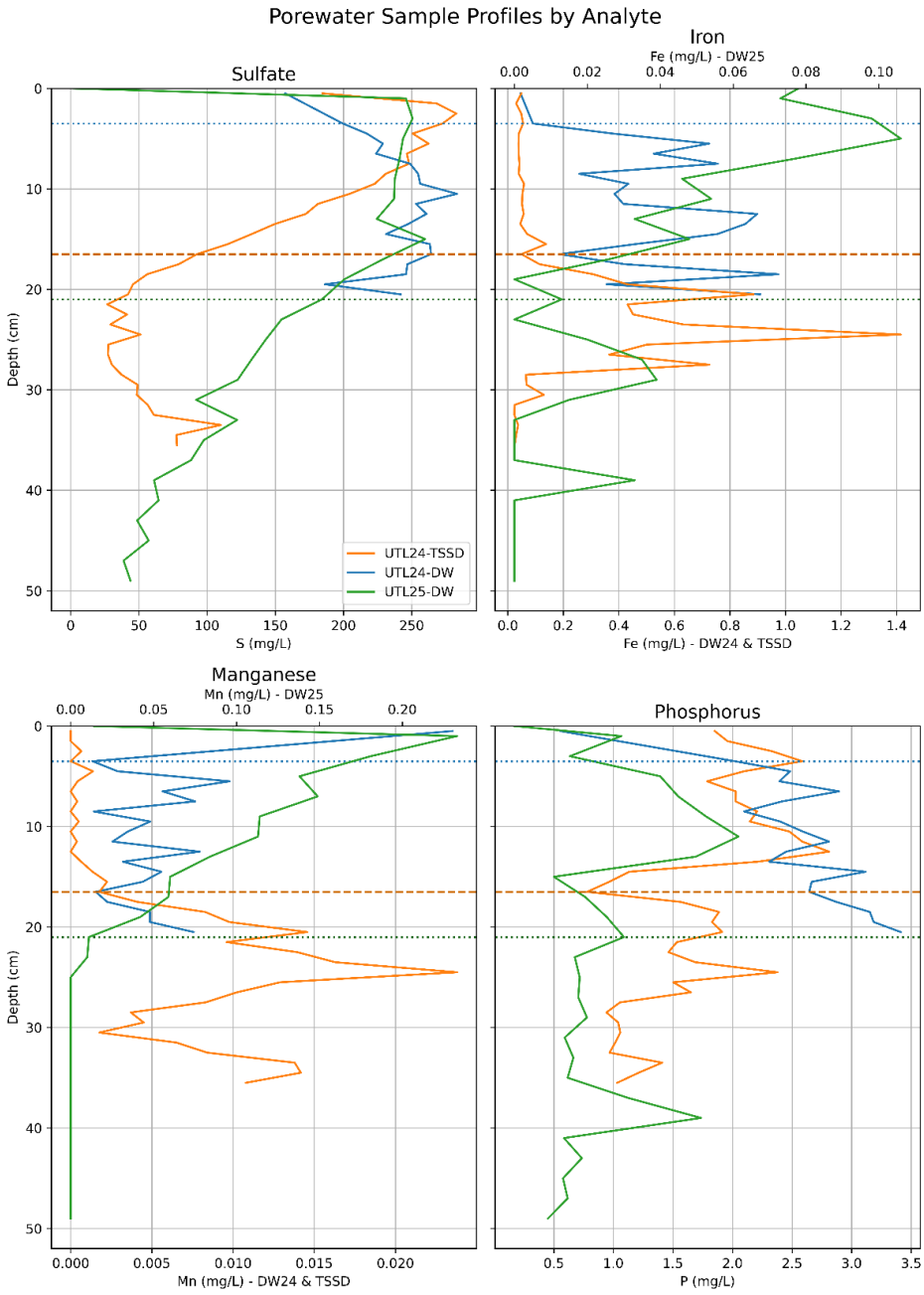

Figure 12

These graphs exhibit a porewater geochemistry comparison between the cores. The dashed orange line shows approximately where maximum sulfate reduction may be occurring for UTL24-TSSD (typical Eh of ~ -200 mV). The dotted green line shows approximately where maximum manganese reduction may be occurring for UTL25-DW (~+200 to +400 mV). This corresponds to a drop in phosphorus levels in the porewater for those cores, potentially indicating the influence of redox in phosphorus release. UTL24-DW was not evaluated due to the limited depth data for that core.

a

Phosphorus Diffusion Results per Core

Core	Gradient Depths (cm)	Slope	Porosity	P in OP ($\frac{mT}{yr}$)	Total P ($\frac{mT}{yr}$)
UTL24-DW	0.5-4.5	0.743	0.667	554	967
UTL24-TSSD	0.5-3.5	0.385	0.769	392	685
UTL25-DW	0.5-12.5	0.484	0.709	411	717
Average ($\frac{mT}{yr}$)				452	790

b

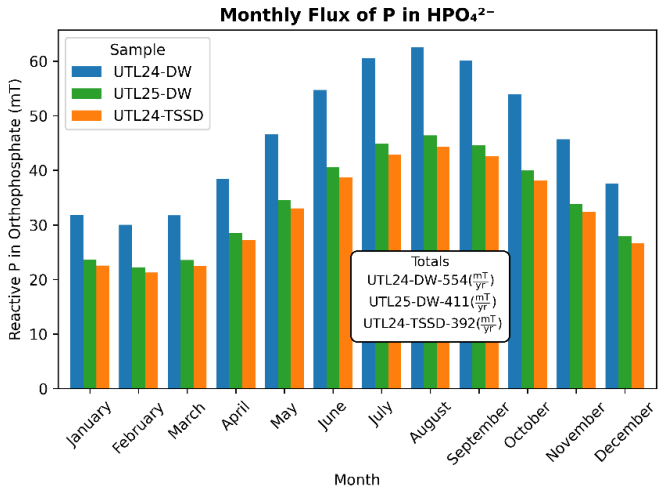

c

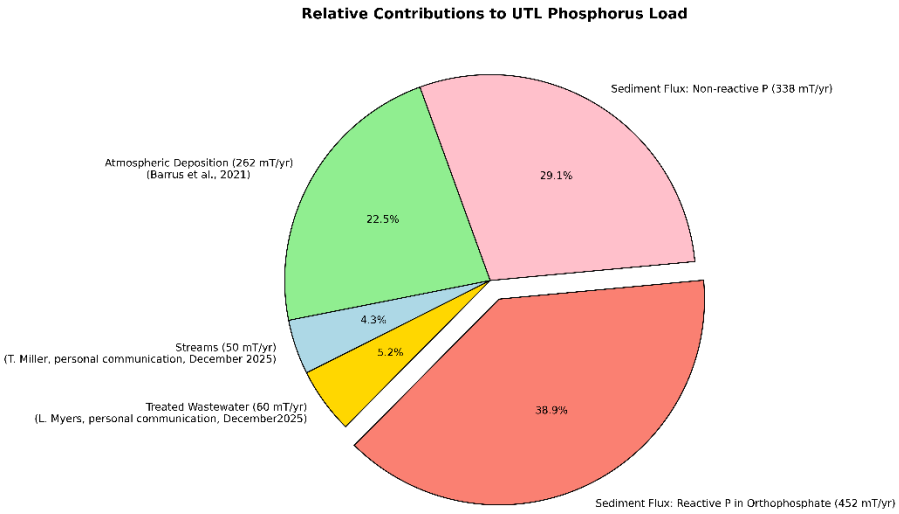

Figure 13

a) This table shows the diffusive phosphorus results for each core based on the first phosphorus gradient and using Fick's first law of diffusion. b) This graph shows how temperature each month influences the fluctuation of phosphorus from the sediment. UTL24-TSSD and UTL25-DW are significantly less than UTL24-DW, most likely due to groundwater influences. c) This pie chart shows how the estimated numbers fit into the estimated UTL phosphorus load budget and the significant contribution of sediment flux heavily outweigh the WWTP contributions.

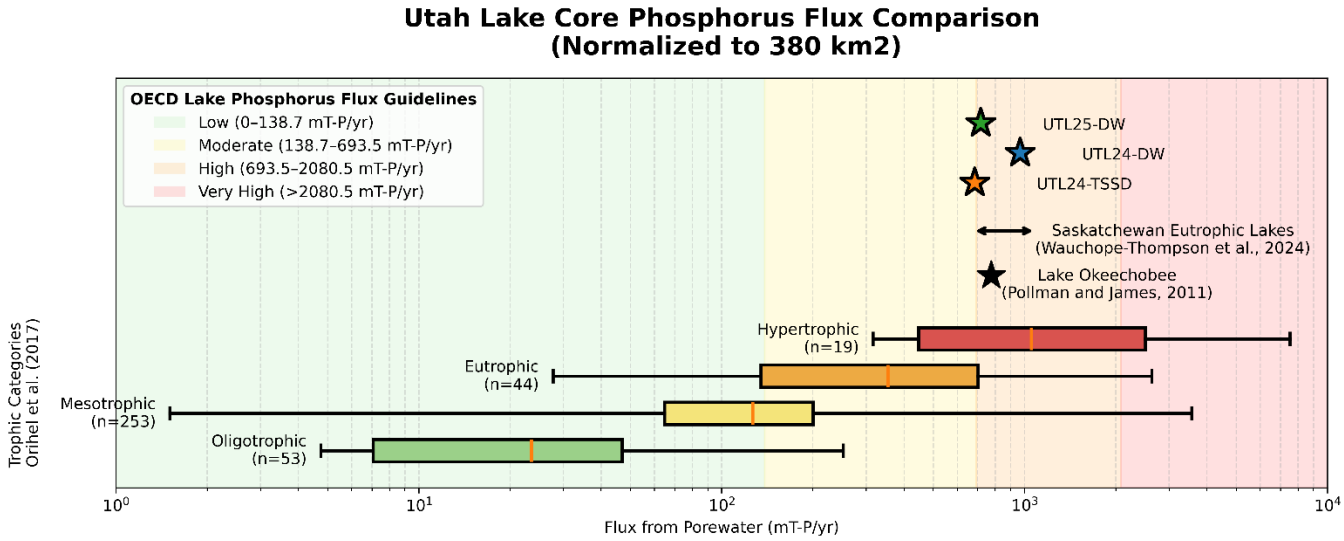

Figure 14

UTL freeze core phosphorus flux comparison to Orihel et al. (2017) Canadian lake data as well as a couple other eutrophic, hardwater lakes for perspective. UTL samples fit within the expected eutrophic bounds and fall in the high range for the Organization of Economic Co-operation and Development (OECD) guidelines.

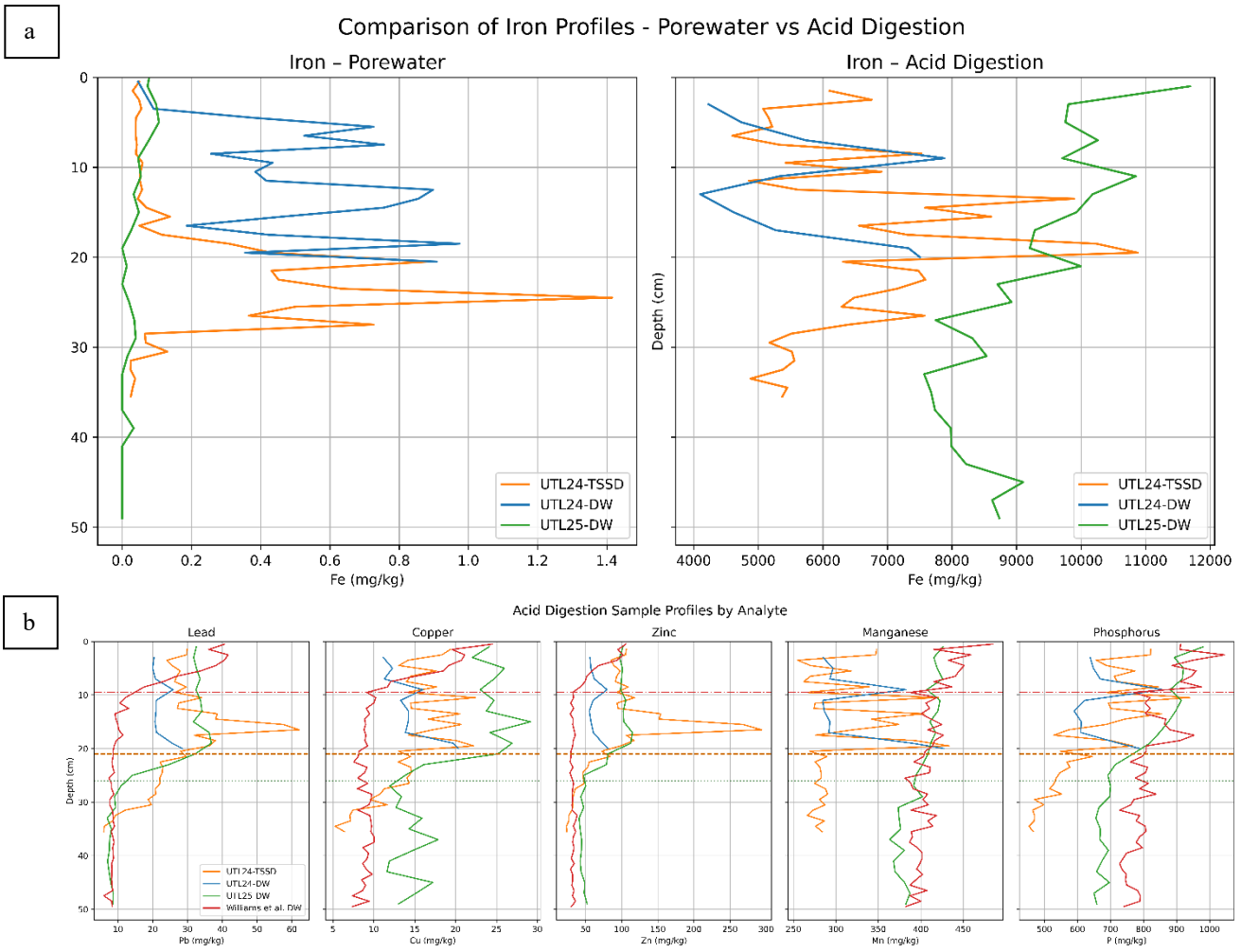

Figure 15

Comparison of porewater and concentration of iron in dry sediment to show a possible effect of porewater extraction via MQ water. b) Comparison of acid digestion concentrations to Williams et al. (2023). Similar increasing patterns could be due to preserved anthropogenic effects but also porewater indicates redox reactions occurring. The variable patterns suggest the lack of deep mixing by resuspension.

REFERENCES

Barrus, S. M., Williams, G. P., Miller, A. W., Borup, M. B., Merritt, L. B., Richards, D. C., & Miller, T. G. (2021). Nutrient atmospheric deposition on Utah Lake: A comparison of sampling and analytical methods. Hydrology, 8(3), 123. https://doi.org/10.3390/hydrology8030123

Baskin, R., Spangler, L., & Holmes, W. (1994). Physical characteristics and quality of water from selected springs and wells in the Lincoln Point-Bird Island area, Utah Lake, Utah. https://doi.org/10.3133/wri934219

Bennett, E. M., Carpenter, S. R., & Caraco, N. F. (2001). Human Impact on erodible phosphorus and eutrophication: A Global perspective. BioScience, 51(3), 227. https://doi.org/10.1641/0006-3568(2001)051

Berg, J. S., Rodriguez, P. C., Magnabosco, C., Deng, L., Bernasconi, S. M., Vogel, H., Morlock, M., & Lever, M. A. (2025). Microbial sulfur cycling across a 13 500-year-old lake sediment record. Biogeosciences, 22(19), 5483–5496. https://doi.org/10.5194/bg-22-5483-2025

Bishop, T. B. B., Brooks, L., Hungerford, H., Utah Valley University, Moser, C., & Stott, A. (2024). Historical overview of territorial, state, and federal legislation impacting Utah Lake. https://www.uvu.edu/herbertinstitute/docs/utah_lake_paper_pre_final_edits.pdf

Brahney, J. (2019). Estimating Total and Bioavailable Nutrient Loading to Utah Lake from the Atmosphere. In Watershed Sciences Faculty Publications (p. 1). Utah State University. https://doi.org/10.15142/em0e-tt24

Carling, G. T., Fernández, D. P., Rudd, A., Pazmiño, E., & Johnson, W. P. (2011). Trace element diel variations and particulate pulses in perimeter freshwater wetlands of Great Salt Lake, Utah. Chemical Geology, 283(1–2), 87–98. https://doi.org/10.1016/j.chemgeo.2011.01.001

Charlton, S.R., Macklin, C.L. and Parkhurst, D.L., 1997. PHREEQCI: A graphical user interface for the geochemical computer program PHREEQC (No. 97-4222). US Geological Survey.

Chen, M., & Q, L., MA. (1998). Comparison of four USEPA digestion methods for trace metal analysis using certified and Florida soils. Journal of Environmental Quality, 27(6), 1294–1300. https://doi.org/10.2134/jeq1998.00472425002700060004x

Cole, J. J., Caraco, N. F., & Likens, G. E. (1990). Short-range atmospheric transport: A significant source of phosphorus to an oligotrophic lake. Limnology and Oceanography, 35(6), 1230–1237. https://doi.org/10.4319/lo.1990.35.6.1230

Ding, S., Wang, Y., Wang, D., Li, Y. Y., Gong, M., & Zhang, C. (2016). In situ, high-resolution evidence for iron-coupled mobilization of phosphorus in sediments. Scientific Reports, 6(1), 24341. https://doi.org/10.1038/srep24341

Fisher, M., & Reddy, K. (2013). Soil pore water sampling methods. In Soil Science Society of America book series (pp. 55–70). https://doi.org/10.2136/sssabookser10.c4

FOX 13 News Utah (KSTU). (2016, February 24). FOX 13 News Utah (KSTU). https://www.fox13now.com/2016/02/22/ancient-bacteria-in-utah-waters-blamed-for-deaths-of-pets-people

Goodman, M. M., Carling, G. T., Fernández, D. P., Rey, K. A., Hale, C. A., Bickmore, B. R., Nelson, S. T., & Munroe, J. S. (2019). Trace element chemistry of atmospheric deposition along the Wasatch Front (Utah, USA) reflects regional playa dust and local

urban aerosols. Chemical Geology, 530, 119317. https://doi.org/10.1016/j.chemgeo.2019.119317

GPM Enviro Project Manager, LLC. (2025, June). Utah Department of Environmental Quality-Water Quality. Retrieved November 19, 2025, from https://deq.utah.gov/businesses-facilities/gpm-enviro-project-manager

Hahnenberger, M., & Nicoll, K. (2012). Meteorological characteristics of dust storm events in the eastern Great Basin of Utah, U.S.A. Atmospheric Environment, 60, 601–612. https://doi.org/10.1016/j.atmosenv.2012.06.029

Harris, E. (2023, December). State and County Population Estimates for Utah: 2022. Kem C. Gardner Policy Institute, University of Utah. https://gardner.utah.edu/wp content/uploads/UPC-Estimates-Dec2023.pdf

Heinrich, L., Dietel, J., & Hupfer, M. (2021). Sulphate reduction determines the long-term effect of iron amendments on phosphorus retention in lake sediments. Journal of Soils and Sediments, 22(1), 316–333. https://doi.org/10.1007/s11368-021-03099-3

Ho, J. C., Michalak, A. M., & Pahlevan, N. (2019). Widespread global increase in intense lake phytoplankton blooms since the 1980s. Nature, 574(7780), 667–670. https://doi.org/10.1038/s41586-019-1648-7

Hoffman, K. (2019). DWQ Statewide Nutrient Removal Cost Impact Study [Slide show; Online PDF Slides]. Utah Department of Environmental Quality. https://documents.deq.utah.gov/water-quality/locations/utah-lake/DWQ-2019-009771.pdf

Fuhriman, Dean K.; Merritt, Lavere B.; Miller, A. Woodruff; and Stock, Harold S. (1981) "Hydrology and water quality of Utah Lake," Great Basin Naturalist Memoirs: Vol. 5 , Article 4.

Jackson, R. H., & Stevens, D. J. (1981). Physical and cultural environment of Utah Lake and adjacent areas. ScholarsArchive (Brigham Young University), 5(1), 2. https://scholarsarchive.byu.edu/gbnm/vol5/iss1/2

Jarvis, F. F. S. (2023). Phosphorus Sorption and Kinetics Across the Sediment-Water Interface of Utah Lake, Shallow Eutrophic Lake. Brigham Young University Theses and Dissertations, 10499. https://scholarsarchive.byu.edu/cgi/viewcontent.cgi?article=11508&context=etd

King, L., Brahney, J., Daly, S., Paul, M. J., Salk, K. R., & Brothers, S. (2023). Primary production modeling identifies restoration targets for shifting shallow, eutrophic lakes to clear-water regimes. Freshwater Science, 42(1), 44–57. https://doi.org/10.1086/723892

Komor, S. C. (1992). Bidirectional sulfate diffusion in saline-lake sediments: Evidence from Devils Lake, northeast North Dakota. Geology, 20(4), 319. https://doi.org/10.1130/0091-7613(1992)020

LeMonte, J. J., Jarvis, F. F. S., Aremu, A., Hughes, A., Hunter, K., Hales, K., Overson, M., Nelson, S. T., Rey, K. A., & Carling, G. T. (2023). Utah Lake Sediment Phosphorus Binding Findings Report. Utah Division of Water Quality.

Li, Y., & Gregory, S. (1974). Diffusion of ions in sea water and in deep-sea sediments. Geochimica Et Cosmochimica Acta, 38(5), 703–714. https://doi.org/10.1016/0016-7037(74)90145-8

Marcy, M., Carling, G. T., Thompson, A. M., Bickmore, B. R., Nelson, S. T., Rey, K. A., Fernández, D. P., Heiner, M., & Adams, B. L. (2024). Trace element chemistry and strontium isotope ratios of atmospheric particulate matter reveal air quality impacts from mineral dust, urban pollution, and fireworks in the Wasatch Front, Utah, USA. Applied Geochemistry, 162, 105906. https://doi.org/10.1016/j.apgeochem.2024.105906

Matsuzaki, S. S., Usio, N., Takamura, N., & Washitani, I. (2007). Effects of common carp on nutrient dynamics and littoral community composition: roles of excretion and bioturbation. Fundamental and Applied Limnology / Archiv Für Hydrobiologie, 168(1), 27–38. https://doi.org/10.1127/1863-9135/2007/0168-0027

Miller, T. Misrepresentations of The Utah Lake Nutrient Budget: Science Panel Decisions To Deny Empirical Data. In Proceedings of Utah Lake Science Panel Meeting, Salt Lake CIty, UT, June.

Munroe, J. S., Carling, G. T., Perry, K. D., Fernandez, D. P., & Mallia, D. V. (2025). Mixing of natural and urban dust along the Wasatch Front of northern Utah, USA. Scientific Reports, 15(1), 3851. https://doi.org/10.1038/s41598-025-88529-9

Neff, J.C., Ballantyne, A.P., Farmer, G.L., Mahowald, N.M., Conroy, J.L., Landry, C.C., Overpeck, J.T., Painter, T.H., Lawrence, C.R. and Reynolds, R.L., 2008. Increasing eolian dust deposition in the western United States linked to human activity. Nature Geoscience, 1(3), pp.189-195.

Nelson, S. T., & Smith, K. E. (2024). Report on Diatom Stratigraphy and Phosphorus Diffusive Fluxes from Utah Lake Freeze Cores near the State Park Buoy, as Well as the Fraction of Soluble P from Dust. Wasatch Front Water Quality Council.

Olsen, J. M., Williams, G. P., Miller, A. W., & Merritt, L. B. (2018). Measuring and calculating current atmospheric phosphorous and nitrogen loadings to Utah Lake using field samples and geostatistical analysis. Hydrology, 5(3), 45. https://doi.org/10.3390/hydrology5030045

Oviatt, C. G. (2015). Chronology of Lake Bonneville, 30,000 to 10,000 yr B.P. Quaternary Science Reviews, 110, 166–171. https://doi.org/10.1016/j.quascirev.2014.12.016

Paerl, H. W., & Otten, T. G. (2013). Harmful cyanobacterial blooms: Causes, consequences, and controls. Microbial Ecology, 65(4), 995–1010. https://doi.org/10.1007/s00248-012-0159-y

Pollman, C. D., & James, R. T. (2011). A simple model of internal loading of phosphorus in Lake Okeechobee. Lake and Reservoir Management, 27(1), 15–27. https://doi.org/10.1080/07438141.2010.542877

PSOMAS & SWCA. (2007). Utah Lake TMDL: Pollutant Loading Assessment and Designated Beneficial Use Impairment Assessment. In Utah Division of Water Quality. Utah Division of Water Quality.

Randall, M., Carling, G. T., Dastrup, D. B., Miller, T. G., Nelson, S. T., Rey, K. A., Hansen, N. C., Bickmore, B. R., & Aanderud, Z. T. (2019). Sediment potentially controls in-lake phosphorus cycling and harmful cyanobacteria in shallow, eutrophic Utah Lake. PLOS ONE, 14(2), e0212238. https://doi.org/10.1371/journal.pone.0212238

Richards, D. C., & Miller, T. (2022). Supplemental carp control method for Utah Lake. Wasatch Front Water Quality Council. Retrieved November 15, 2025, from https://www.researchgate.net/publication/362290147_Supplemental_carp_control_method_for_Utah_Lake?enrichId=rgreq-9cd19d41feee94767fb5a05665d45154-XXX&enrichSource=Y292ZXJQYWdlOzM2MjI5MDE0NztBUzoxMTgyNDU2MzE3MjQ3NTAwQDE2NTg5MzA5NjM5OTA%3D&el=1_x_2

Schindler, D. W. (1974). Eutrophication and recovery in Experimental lakes: Implications for Lake Management. Science, 184(4139), 897–899. https://doi.org/10.1126/science.184.4139.897

Schindler, D. W., Carpenter, S. R., Chapra, S. C., Hecky, R. E., & Orihel, D. M. (2016). Reducing Phosphorus to Curb Lake Eutrophication is a Success. Environmental Science & Technology, 50(17), 8923–8929. https://doi.org/10.1021/acs.est.6b02204

Steenburgh, W. J., Massey, J. D., & Painter, T. H. (2012). Episodic dust events of Utah's Wasatch Front and adjoining region. Journal of Applied Meteorology and Climatology, 51(9), 1654–1669. https://doi.org/10.1175/jamc-d-12-07.1

Savitz, J. D., Campbell, C., Wiles, R., Hartmann, C. (1996). "Dishonorable Discharge: Toxic Pollution of Utah Waters." Environmental Working Group, https://static.ewg.org/files/DD_PDF/UT.pdf.

Taggart, J. B., Woodland, L. M., Tanner, K. B., & Williams, G. P. (2025). A Geochemical Study of Near-Shore Sediment Cores from Utah Lake, UT, USA. Geosciences, 15(9), 363. https://doi.org/10.3390/geosciences15090363

Tate, R. S. (2019). Landsat Collections Reveal Long-Term Algal Bloom Hot Spots of Utah Lake [MS Thesis, Brigham Young University]. https://scholarsarchive.byu.edu/cgi/viewcontent.cgi?article=9585&context=etd

Telfer, J. T., Brown, M. M., Williams, G. P., Tanner, K. B., Miller, A. W., Sowby, R. B., & Miller, T. G. (2023). Source Attribution of atmospheric dust deposition to Utah Lake. Hydrology, 10(11), 210. https://doi.org/10.3390/hydrology10110210

Utah Department of Environmental Quality-Air Quality. (2023). Utah PM10 concentration adjusted to sea level. In https://air.utah.gov/dataarchive/archpm10.htm. DEQ-Air Quality. Retrieved January 8, 2025, from https://air.utah.gov/dataarchive/PM10NOV23.pdf

Utah Department of Environmental Quality, Division of Water Quality. (2025, January 9). Utah Lake Water Quality Study Steering Committee meeting summary (DRAFT) [Virtual meeting]. Retrieved November 9, 2025, from https://lf-public.deq.utah.gov/WebLink/ElectronicFile.aspx?docid=529471&eqdocs=DWQ-2025-00

Utah Division of Water Quality. (2014). Phosphorus Rule Fact Sheet. In Utah Department of Environmental Quality. Utah Department of Environmental Quality. Retrieved September 20, 2023, from https://documents.deq.utah.gov/legacy/topics/fact-sheet/docs/handouts/phosphorusfactsheet.pdf

Utah Division of Water Resources. (2014). Utah Lake Basin- Planning for the Future. In www.water.utah.gov. Retrieved June 4, 2025, from https://water.utah.gov/wp-content/uploads/2019/SWP/UtahLake/UtahLake2014.pdf

VanCuren, R., Pederson, J., Lashgari, A., Dolislager, L., & McCauley, E. (20012). Aerosol generation and circulation in the shore zone of a Large Alpine lake – 2 – Aerosol distributions over Lake Tahoe, CA. Atmospheric Environment, 46, 631–644. https://doi.org/10.1016/j.atmosenv.2009.08.049

Waterisotopes Database. (2022). http://waterisotopesDB.org. Accessed 11/2024. Query: Country=US, State=UT, Type=Ground

Wauchope-Thompson, M. S., Baulch, H. M., & Cade-Menun, B. J. (2024). Internal phosphorus loading in a chain of eutrophic hardwater lakes in Saskatchewan, Canada. The Science of the Total Environment, 924, 171493. https://doi.org/10.1016/j.scitotenv.2024.171493

Williams, R., Nelson, S. T., Rushforth, S. R., Rey, K. A., Carling, G. T., Bickmore, B. R., Heathcote, A. J., Miller, T. G., & Meyers, L. (2023). Human-Driven Trophic Changes in a Large, Shallow Urban Lake: Changes in Utah Lake, Utah from Pre-European Settlement to the Present. Water, Air, & Soil Pollution, 234(4). https://doi.org/10.1007/s11270-023-06228-5

Yuan, Z., Jiang, S., Sheng, H., Liu, X., Hua, H., Liu, X., Zhang, Y., Yuan, Z., Jiang, S., Sheng, H., Liu, X., Hua, H., Liu, X., & Zhang, Y. (2018). Human perturbation of the global phosphorus Cycle: changes and consequences. Environmental Science & Technology, 52(5), 2438–2450. https://doi.org/10.1021/acs.est.7b03910

Zanazzi, A., Wang, W., Peterson, H., & Emerman, S. H. (2020). Using stable isotopes to determine the water balance of Utah Lake (Utah, USA). Hydrology, 7(4), 88. https://doi.org/10.3390/hydrology7040088

40 CFR appendix L to part 50 - Appendix L to Part 50—Reference method for the determination of fine particulate matter as PM2.5 in the atmosphere. (n.d.). LII / Legal Information Institute. https://www.law.cornell.edu/cfr/text/40/appendix-L_to_part_50